Molecular Pharmacology Fast Forward. Published on November 2, 2010 as doi:10.1124/mol.110.069013
This article has not been copyedited and formatted. The final version may differ from this version.

MOL #69013

MRP1 FUNCTION AND LOCALIZATION DEPEND ON CORTICAL ACTIN

Ina Hummel, Karin Klappe, Cigdem Ercan, and Jan Willem Kok

Department of Cell Biology, Section Membrane Cell Biology, University Medical Center Groningen, University of Groningen, A. Deusinglaan 1, 9713 AV Groningen, The Netherlands

Running title: Cortical actin stabilizes Mrp1/MRP1 function

Address correspondence to: Jan Willem Kok, University Medical Center Groningen, University of Groningen, Department of Cell Biology, Section Membrane Cell Biology, A. Deusinglaan 1, 9713 AV Groningen, The Netherlands, Tel. 31-50-3632725; Fax 31-50-3632728; E-mail: j.w.kok@med.umcg.nl

Number of text pages: 37
Number of tables: 0
Number of figures: 13
Number of references: 22
Number of words in *Abstract*: 204
Number of words in *Introduction*: 739
Number of words in *Discussion*: 709

Abbreviations: ABC, ATP-binding cassette; Cav-1, caveolin-1; CFDA, 5-carboxyfluorescein diacetate; LC-ESI-MS/MS, liquid chromatography-electrospray ionization tandem mass spectrometry; MDR, multidrug resistance; Mrp1, murine multidrug resistance-related protein 1; MRP1, human multidrug resistance-related protein 1; PGP/Pgp, P-glycoprotein

Molecular Pharmacology Fast Forward. Published on November 2, 2010 as DOI: 10.1124/mol.110.069013
This article has not been copyedited and formatted. The final version may differ from this version.

ABSTRACT

MRP1 (ABCC1) is known to be localized in lipid rafts. Here we show in two different cell lines that localization of Mrp1/MRP1 (Abcc1/ABCC1) in lipid rafts and its function as an efflux pump are dependent on cortical actin. Latrunculin B disrupts both cortical actin and actin stress fibres. This results in partial loss of actin and Mrp1/MRP1 (Abcc1/ABCC1) from detergent-free lipid raft fractions, partial internalization of Mrp1/MRP1 (Abcc1/ABCC1) and reduction of Mrp1/MRP1 (Abcc1/ABCC1)-mediated efflux. Pretreatment with nocodazole prevents latrunculin B-induced loss of cortical actin and all effects of latrunculin B on Mrp1 (Abcc1) localization and activity. However, pretreatment with tyrphostin A23 does not prevent latrunculin B-induced loss of cortical actin, lipid raft association and efflux activity, but does prevent latrunculin B-induced internalization of Mrp1 (Abcc1). Cytochalasin D disrupts actin stress fibres but not cortical actin and this inhibitor much less affects Mrp1/MRP1 (Abcc1/ABCC1) localization in lipid rafts, internalization and efflux activity. In conclusion, cortical actin disruption results in reduced Mrp1/MRP1 (Abcc1/ABCC1) activity concomitant with a partial shift of Mrp1/MRP1 (Abcc1/ABCC1) out of lipid raft fractions and partial internalization of the ABC transporter. The results suggest that reduced Mrp1 (Abcc1) function is correlated to loss of lipid raft association but not internalization of Mrp1 (Abcc1).

Molecular Pharmacology Fast Forward. Published on November 2, 2010 as DOI: 10.1124/mol.110.069013
This article has not been copyedited and formatted. The final version may differ from this version.

INTRODUCTION

One of the best characterized multidrug resistance (MDR) mechanisms is the overexpression of ATP-binding cassette (ABC) transporter proteins, which prevent intracellular drug accumulation. Among these proteins, P-glycoprotein (PGP/Pgp or ABCB1/ Abcb1) and multidrug resistance-related protein 1 (Mrp1/MRP1 or Abcc1/ABCC1) are the most widely studied. Both ABC transporters are known to depend on their direct lipid environment in model membranes for optimal functioning (Dudeja *et al.*, 1995; Sinicrope *et al.*, 1992). Pgp (Abcb1) was found to have a higher affinity for its substrates when the surrounding lipids are in the liquid-ordered phase rather than in the liquid-disordered phase (Romsicki and Sharom, 1999). The liquid-ordered phase occurs when lipids have a high degree of saturation, like sphingolipids, which enables them to pack tightly. This is a putative characteristic of membrane microdomains or lipid rafts (including caveolae) in living cells as well (Brown and London, 2000; Schroeder *et al.*, 1994).

Lavie *et al.* (1998) have shown for the first time the association of an ABC transporter with a membrane domain. They found that a substantial fraction of PGP (ABCB1) in Pgp (ABCB1) overexpressing cells was located in Triton X-100-based detergent-resistant membranes, containing caveolin 1 (Cav-1). On the other hand, it was shown that PGP (ABCB1) and MRP1 (ABCC1) were not associated with caveolae in two human MDR tumor cell lines. Both MRP1 (ABCC1) and PGP (ABCB1) were found to be enriched in membrane domains defined by their insolubility in the non-ionic detergent Lubrol. In 2780AD cells PGP (ABCB1) was located in non-caveolar detergent-resistant membranes, since these cells did not express Cav-1 and hence lack caveolae. $HT29^{col}$ cells did express Cav-1, but MRP1 (ABCC1) and Cav-1 did not colocalize and were not coimmunoprecipitated (Hinrichs *et al.*, 2004). Another study also reported dissociation of Pgp (Abcb1) from caveolae in a MDR Chinese hamster ovary cell line and postulated that Pgp (Abcb1) resides in an intermediate-

Molecular Pharmacology Fast Forward. Published on November 2, 2010 as DOI: 10.1124/mol.110.069013
This article has not been copyedited and formatted. The final version may differ from this version.

density membrane microdomain which is distinct from both caveolar domains and classical lipid rafts, and which is defined by insolubility in Brij-96 (decaethoxy oleoyl ether) (Radeva *et al.*, 2005).

Formation and maintenance of lipid rafts appear to depend on specific lipids, namely sphingolipids and cholesterol. Lipid rafts are often considered to be highly dynamic entities, which may arise and dissolve continuously. On the other hand, the actin cytoskeleton appears to have the potential to stabilize them, at least temporarily. In fact, cortical actin may confer dynamic properties on lipid rafts, stabilizing them as separate domains upon actin binding while the lipid rafts are able to move laterally and coalesce when disconnected from the actin cytoskeleton (Chichili and Rodgers, 2007). Interestingly, PGP (ABCB1) has been shown to be partially linked to the actin cytoskeleton (Bacso *et al.*, 2004). Moreover, PGP (ABCB1)-actin association through ezrin, radixin and moesin (ERM family proteins) has been shown in a MDR variant of a human T-lymphoblastoma cell line CEM-VBL100. Down-regulation of all three ERM proteins resulted in loss of PGP (ABCB1)-actin association, PGP (ABCB1) redistribution and concomitant sensitization to vinblastine, which accumulated due to reduction of PGP (ABCB1)-mediated drug efflux. These data indicate that the ERM protein-mediated link between PGP (ABCB1) and F-actin is functional in MDR (Luciani *et al.*, 2002). Another example of ABC transporter-actin associations mediated by ERM proteins is the direct association of radixin with the carboxy-terminal cytoplasmic domain of human MRP2 (ABCC2), which was discovered in $Rdx^{-/-}$ mice (Kikuchi *et al.*, 2002). Radixin deficiency in these mice results in loss of MRP2 (ABCC2) from bile canalicular membranes, which leads to conjugated hyperbilirubinemia, a phenotype very similar to that of Dubin-Johnson syndrome characterized by mutations in *MRP2*/*ABCC2*, encoding MRP2. Thus, the ERM protein radixin in liver cells is essential for the correct localization of MRP2 (ABCC2) and its function in

Molecular Pharmacology Fast Forward. Published on November 2, 2010 as DOI: 10.1124/mol.110.069013
This article has not been copyedited and formatted. The final version may differ from this version.

conjugated bilirubin secretion. However, for the family member Mrp1/MRP1 (Abcc1/ABCC1) no (direct or indirect) link to the actin cytoskeleton is known.

In this study we investigated the impact of disruption of the actin cytoskeleton on the localization of Mrp1/MRP1 (Abcc1/ABCC1) and its efflux function. We studied subcellular localization of Mrp1/MRP1 (Abcc1/ABCC1) by confocal microscopy and its sub-membrane localization by non-detergent lipid raft analysis. Mrp1/MRP1 (Abcc1/ABCC1) function was determined by an efflux assay. We conclude that cortical actin stabilizes Mrp1/MRP1 (Abcc1/ABCC1) efflux activity and its localization in lipid rafts on the cell surface. Studies using tyrphostin A23 to inhibit Mrp1 (Abcc1) internalization suggest that reduction of Mrp1 (Abcc1) function is correlated to loss of lipid raft association, but not internalization, of the ABC transporter.

Molecular Pharmacology Fast Forward. Published on November 2, 2010 as DOI: 10.1124/mol.110.069013
This article has not been copyedited and formatted. The final version may differ from this version.

MATERIALS AND METHODS

Materials

MK571 was a gift from Prof. A.W. Ford-Hutchinson (Merck-Frosst, Inc., Kirkland, Canada). The monoclonal anti-giantin antibody was a gift from Dr. Hauri (Department of Pharmacology, University of Basel, Switzerland). All cell culture plastic was from Costar (Cambridge, MA). RNeasy Mini Kit was obtained from Qiagen (Valencia, CA). Cell culture media, Hank's balanced salt solution (HBSS), antibiotics, L-glutamine, sodium pyruvate, trypsin, Platinum Blue PCR SuperMix, primers and all reagents for reverse transcription were from Invitrogen (Paisley, UK). Fetal calf serum (FCS) was from Bodinco (Alkmaar, The Netherlands). Latrunculin B, cytochalasin D, nocodazole, 5-carboxy-fluorescein diacetate, rhodamine 123, TRI reagent, and the monoclonal anti-β-actin antibody were obtained from Sigma-Aldrich (St. Louis, MO). Cyclosporin A was from Alexis (Carlsbad, CA). Jasplakinolide was from Calbiochem (La Jolla, CA). Tyrphostin A23 was obtained from Santa Cruz Biotechnology Inc. (Santa Cruz, CA). Phalloidin Alexa Fluor 488 and 633 and all Alexa Fluor-conjugated secondary antibodies were obtained from Molecular probes (Eugene, OR). OptiPrep was from Axis-Shield PoC AS (Dundee, Scotland). C12-fatty acid homologues of ceramide, sphingomyelin, glucosylceramide and lactosylceramide were from Avanti Polar Lipids (Alabaster, AL). The rat monoclonal anti-MRP1 (ABCC1) (MRPr1) antibody was obtained from Signet Laboratories (Dedham, MD). The polyclonal anti-Cav-1 antibody was from Transduction Laboratories (Lexington, KY). The monoclonal anti-transferrin receptor antibody was from Zymed (San Francisco, CA).

Cell culture and incubation conditions

The murine neuroblastoma cell line Neuro-2a was purchased from the ATCC (Manassas, VA, USA). These cells were grown as adherent monolayer cultures in Dulbecco's modified Eagle

Molecular Pharmacology Fast Forward. Published on November 2, 2010 as DOI: 10.1124/mol.110.069013
This article has not been copyedited and formatted. The final version may differ from this version.

medium supplemented with 10% FCS, 100 units/ml penicillin, 100 µg/ml streptomycin, 2 mM L-glutamine and 1 mM sodium pyruvate, under standard incubator conditions (humidified atmosphere, 5% CO_2, 37°C). The hamster BHK cell line stably expressing the human *MRP1/ABCC1* gene, named BHK-MRP1, was a gift from Dr. Riordan (Mayo Clinic Arizona, S.C. Johnson Medical Research Center, Scottsdale, AZ, USA; Chang *et al.*, 1997). These cells were grown as adherent monolayer cultures in Dulbecco's modified Eagle medium/NUT mix F-12 (1:1) supplemented with 10% FCS, 100 units/ml penicillin, 100 µg/ml streptomycin and 2 mM L-glutamine, under standard incubator conditions (humidified atmosphere, 5% CO_2, 37^{o}C). The cells were kept under selective pressure by growing them in the presence of 100 µM methotrexate. In order to disrupt the actin cytoskeleton, cells were treated with 10 µg/ml cytochalasin D or 10 µM latrunculin B for 35 minutes. In some cases, cells were preincubated with 10 µM nocodazole for 45 minutes to disrupt microtubules, followed by treatment with both nocodazole and latrunculin B for 35 minutes. Alternatively, cells were pre- and co-treated with 300 µM tyrphostin A23. In some experiments, cells were treated with 50 nM jasplakinolide for 20h. All incubations with cytoskeleton modulators and all control experiments without these modulators were performed in medium without serum to avoid binding of the modulators to serum factors.

Isolation of detergent-free lipid rafts

Neuro-2a cells were plated at a density of $2x10^5$ cells/ml and BHK-MRP1 at $2.5x10^5$ cells/ml, one day prior to the experiment. Detergent-free lipid rafts were isolated as described (Macdonald and Pike, 2005). The whole procedure was performed on ice. In short, confluent cells of two 75 cm^2 flasks were washed with base buffer (20 mM Tris-HCl pH 7.8, 250 mM sucrose) supplemented with 1 mM $CaCl_2$ and 1 mM $MgCl_2$. The cells were collected by scraping in this solution and centrifuged for 2 minutes at 250g. The resulting pellet was

Molecular Pharmacology Fast Forward. Published on November 2, 2010 as DOI: 10.1124/mol.110.069013
This article has not been copyedited and formatted. The final version may differ from this version.

dissolved in 1 ml of base buffer supplemented with 1 mM $CaCl_2$, 1 mM $MgCl_2$ and protease inhibitors. After homogenization by passage through a 25 Gauge needle 20 times, another centrifugation step for 10 minutes at 1000g followed. The resulting post nuclear supernatant (PNS) was collected and transferred to a separate tube. The pellet was homogenized again in 1 ml base buffer supplemented with 1 mM $CaCl_2$, 1 mM $MgCl_2$ and protease inhibitors, sheered through the needle 20 times and centrifuged. The second PNS was combined with the first. Protein content of the combined PNS was determined (Smith *et al.*, 1985) and an equal amount of protein per sample was taken and adjusted to 2 ml volume. Subsequently, 2 ml of base buffer containing 50% OptiPrep was added to this 2 ml PNS. By using a gradient mixer, 8 ml gradient of 0% to 20% OptiPrep in base buffer was applied on top of this 4 ml in a centrifugation tube. After centrifugation for 90 minutes at 22,000 rpm and 4^{o}C in a Beckman SW41 rotor (Beckman Coulter, Inc., Fullerton, CA, USA) 9 fractions of 1,34 ml were collected (from top to bottom) and stored at -80^{o}C.

Immunoblot analysis

Protein from equal volumes of the gradient fractions was TCA-precipitated and resuspended in sample buffer (5% SDS, 5% β-mercaptoethanol, 0.125M Tris-HCL pH 6.8, 40% glycerol). The samples were resolved on SDS-PAGE (10%) minigels and subsequently electro transferred onto a nitrocellulose membrane (Trans-Blot Transfer Medium membrane, Bio-Rad, Hercules, CA, USA). The membranes were rinsed with PBS and incubated (1h, RT) with Odyssey blocking buffer/PBS (1:1, v/v). Membranes were incubated (overnight, 4^{o}C) with a primary antibody against MRP1 (ABCC1) (1:1000), Cav-1 (1:1000), or actin (1:5000) in Odyssey blocking buffer/PBS (1:1, v/v), containing 0.1% (v/v) Tween 20 . Membranes were rinsed in washing buffer (PBS containing 0.1% (v/v) Tween 20) and subsequently incubated for 1h with the appropriate IR dye-conjugated secondary antibody (1:5000) (LI-COR,

Molecular Pharmacology Fast Forward. Published on November 2, 2010 as DOI: 10.1124/mol.110.069013
This article has not been copyedited and formatted. The final version may differ from this version.

Westburg, Leusden, The Netherlands) in Odyssey blocking buffer/PBS (1:1, v/v), containing 0.1% (v/v) Tween 20. After rinsing with washing buffer followed by PBS, the immunoblots were scanned with the Odyssey (LI-COR, Westburg, Leusden, The Netherlands) to visualize the immunoreactive complexes, according to the manufacturer's instructions. Relative quantification of the complexes was performed using the Odyssey software.

Analysis of cholesterol, sphingolipid and protein content of OptiPrep gradient fractions

Lipids were extracted from pooled OptiPrep gradient fractions (Bligh and Dyer, 1959). In the extract the cholesterol concentration was determined spectrophotometrically by a cholesterol oxidase/peroxidase assay (Gamble *et al.*, 1978). Sphingolipids were analyzed by liquid chromatography-electrospray ionization tandem mass spectrometry (LC-ESI-MS/MS) on a PE-Sciex API 3000 triple quadrupole mass spectrometer equipped with a turbo ionspray source as described previously (Sullards and Merrill, 2001). HPLC separation was performed as described previously (Sullards *et al.*, 2003), with the following changes: an APS-2 Hypersil 150x2.1 mm column (Thermo Electron, Breda, The Netherlands) was used and the flow rate was 200 µl/min. N_2 was used as the nebulizing gas and drying gas for the turbo ionspray source. The ion spray needle was held at 5,500 V, and the orifice and ring voltages were kept low (30 and 150 V, respectively) to prevent collisional decomposition of molecular ions before entry into the first quadrupole; the orifice temperature was set to 500°C. N_2 was used to collisionally induce dissociations in Q2. Multiple reaction monitoring scans were acquired by setting Q1 and Q3 to pass the precursor and product ions of the most abundant sphingolipid molecular species. MRM transitions and collision energies for each species were taken from table 1 in Sullards *et al.* (2003). The transitions correspond to ceramides, glucosylceramides, lactosylceramides and sphingomyelins with a d18:1 sphingoid base (sphingosine) and C16:0, DHC16:0, C18:0, C20:0, C22:0, C24:1, C24:0, C26:1, and C26:0

Molecular Pharmacology Fast Forward. Published on November 2, 2010 as DOI: 10.1124/mol.110.069013
This article has not been copyedited and formatted. The final version may differ from this version.

fatty acids, respectively. Quantitation was achieved by spiking the samples before extraction with the C12-fatty acid homologues of ceramide, glucosylceramide, lactosylceramide and sphingomyelin. The amounts of individual sphingolipid species were added to obtain the total sphingolipid pool. Protein content of pooled OptiPrep gradient fractions was determined as described by Smith *et al.* (1985).

Reverse transcriptase-polymerase chain reaction (RT-PCR)

Total RNA was isolated from cells by using RNeasy Mini Kit according to the manufacturer's instructions. Total RNA was isolated from murine liver and kidney using TRI reagent according to the manufacturer's instructions. Single-stranded cDNA was synthesized from 1 µg RNA by using 0.5 µg Oligo $(dT)_{12-18}$ primer, 200 units Superscript RT, 4 µl 5× First Strand Buffer, 10 mM 1,4-dithiothreitol (DTT), and 0.5 mM of each dNTP in a total volume of 20 µl. The RNA sample + Oligo $(dT)_{12-18}$ primer were denatured at 65ºC for 15 min and placed on ice for 5 min, before adding it to the reaction. Reverse transcription was performed for 1 h at 37ºC, and the samples were subsequently heated for 5 min at 99ºC to terminate the reverse transcription reaction. PCR was performed with Platinum Blue PCR SuperMix, using 1 µl of the obtained cDNA and 250 nM of each of the appropriate sense and antisense primers, according to the manufacturer's instructions. The final reaction volume was 25 µl. The tubes were incubated in a GeneAmp PCR System 9700 (Perkin-Elmer, Norwalk, CT) at 94ºC for 5 min to denature the primers and cDNA. The cycling program was 94ºC for 30 s, 55ºC for 30 s, and 72ºC for 45 s. The number of cycles was 35 for ABC transporters and 30 for β-actin. The following primer sequences were used (GenBank [GB] accession numbers and nucleotide positions in brackets): Mrp1 sense (GB AF022908 [248-276]) 5'-GGCAGACCTCTTCTACTCT-3', antisense (GB AF022908 [834-815]) 5'-GGCATACACAATCCGTACAG-3' (576 bp amplified product); Mrp2 sense (GB BC172749

Molecular Pharmacology Fast Forward. Published on November 2, 2010 as DOI: 10.1124/mol.110.069013
This article has not been copyedited and formatted. The final version may differ from this version.

[268-292]) 5'-AGCCATAGACCTGTCTCTTGCACTC-3', antisense (GB BC172749 [892-868]) 5'-GACAAGGACATCTTGGCTCTGACTC-3' (624 bp amplified product); Mrp3 sense (GB BC150788 [227-248]) 5'-CATCAGCTCGGCTACATAGTCC-3', antisense (GB BC150788 [799-778]) 5'-AGAGCAGTCCTCCTCAGACAGA-3' (572 bp amplified product); Mrp4 sense (GB BC150822 [161-180]) 5'-ACTGGTCATAAGCGGAGACT-3', antisense (GB BC150822 [476-457]) 5'-CGTAGCCATAAGCTGTATGC-3' (315 bp amplified product); Mrp5 sense (GB BC090629 [264-285]) 5'-CAGGTTCCGGAGAACAAGATCG-3', antisense (GB BC090629 [866-845]) 5'-GCAAGTGACCAGGAGCGTACAA-3' (602 bp amplified product); Mrp6 sense (GB BC156560 [483-502]) 5'-GCATCTTGCCAGGAATCAAC-3', antisense (GB BC156560 [833-814]) 5'-TGCAGCTTCTCCTCCATTCT-3' (350 bp amplified product); Mrp7 sense (GB AF417121 [680-698]) 5'-CCTTCCTGTCCTCTGAGAG-3', antisense (GB AF417121 [936-917]) 5'-GGCCAGGTAGCAACATCCAA-3' (256 bp amplified product); Mdr1a sense (GB M33581 [255-274]) 5'-GTTATGCAGGTTGGCTAGAC-3', antisense (GB M33581 [521-502]) 5'-CCTGGATGTAGGCAACTATG-3' (266 bp amplified product); Mdr1b sense (GB BC141363 [241-260]) 5'-GGACAAGCTGTGCATGATTC-3', antisense (GB BC141363 [426-407]) 5'-TCCAGACTGCTGTTGCTGAT-3' (185 bp amplified product); β-actin sense (GB M12481 [304-321]) 5'-AACACCCCAGCCATGTAC-3', antisense (GB M12481 [557-540]) 5'-ATGTCACGCACGATTTCC-3' (254 bp amplified product). Ten microliters of PCR product was loaded onto a 2% agarose gel stained with ethidium bromide.

Detection of Mrp1/MRP1 (Abcc1/ABCC1)*-mediated efflux by flow cytometric analysis*

Neuro-2a cells were plated at a density of $2x10^5$ cells/ml and BHK-MRP1 at $2.5x10^5$ cells/ml, one day prior to the experiment. Cells were harvested by trypsinization, washed with HBSS and incubated with the Mrp1/MRP1 (Abcc1/ABCC1) substrate 5-carboxyfluorescein

Molecular Pharmacology Fast Forward. Published on November 2, 2010 as DOI: 10.1124/mol.110.069013
This article has not been copyedited and formatted. The final version may differ from this version.

diacetate (CFDA; 0.5 μM in HBSS) at 10^{o}C for 60 minutes. Cells were transferred to ice and washed with ice-cold HBSS. In case of the time point 0 min samples, the Mrp1/MRP1 (Abcc1/ABCC1) inhibitor MK571 (20 μM) was added at this point. In other samples, to allow efflux, the cells were incubated at 37^{o}C in absence of MK571 during various time intervals. In case of the inhibitor control, the 37^{o}C incubation was performed in the presence of MK571. All subsequent steps were performed on ice. The efflux of the fluorescent substrate was stopped by cold centrifugation and the cells were resuspended in ice-cold HBSS containing MK571. Alternatively, in some experiments Neuro-2a cells were incubated with the substrate rhodamine 123 (10 μM in HBSS) and the inhibitor cyclosporin A (10 μM) was used. The remaining cell-associated fluorescence was determined by flow cytometric analysis using an Elite^{TM} flow cytometer (Beckman Coulter, Miami, FL). For each sample 5000 events were collected and analyzed using Win-list 5.0 software (Verity Software House Inc., Topsham, ME). With 5000 events clear Gaussian fluorescence distributions were obtained with a calculated error of measurement of 1.4%. In all graphic representations of results, the values express the fluorescense remaining in the cells after a certain time window of efflux at 37^{o}C, as percentage of the fluorescence after loading the cells (= 100%). In the latter case the cells were not allowed to efflux, as they were kept on ice. This was done for all conditions, so the values always indicate the fraction of the initial CFDA load that remains in the cells after a certain time period of efflux at 37^{o}C.

Confocal laser scanning fluorescence microscopy

Neuro-2a cells were plated on glass cover slips in 12-wells plates at a density of 7x10^{4} cells/ml and BHK-MRP1 at 1.5x10^{5} cells/ml, one day prior to the experiment. Cells were fixed with 4% paraformaldehyde (PFA) at RT for 20 min, permeabilized with 0.1% Triton X-100 at RT for 5 min and blocked with 2% FCS in PBS at RT for 30 min prior to antibody

Molecular Pharmacology Fast Forward. Published on November 2, 2010 as DOI: 10.1124/mol.110.069013
This article has not been copyedited and formatted. The final version may differ from this version.

incubation. Alternatively, cells were fixed with cold (-20°C) methanol or acetone on ice for 5 min, washed extensively with PBS, and blocked with 2% FCS in PBS at RT for 30 min prior to antibody incubation. It should be noted that the latter protocol does not require a permeabilization step, since methanol and acetone readily permeabilize cells. Both fixation protocols were compared for all antigens to optimalize the staining procedure for each antigen. For instance, MRP1 staining by primary and (fluorescent) secondary antibodies is much more pronounced after methanol fixation compared to paraformaldehyde fixation. Primary (overnight at 4°C) and secondary (2h at RT) antibody incubations were carried out in PBS. Cells were stained with antibodies against MRP1 (ABCC1) (1:50), Cav-1 (1:100), transferrin receptor (1:100), giantin (1:500) or β-tubulin (1:100) and appropriate ALEXA-conjugated secondary antibodies. Alternatively, F-actin was stained with ALEXA488- or ALEXA633-conjugated phalloidin. After incubations, cells were washed three times with PBS. Analysis of the samples was performed using a TCS Leica SP2 AOBS Confocal Laser Scanner Microscope (Leica, Heidelberg, Germany), equipped with a HCX PL APO 63x 1.4 oil CS objective in combination with Leica Confocal Software. Images were processed using Adobe Photoshop CS3.

Molecular Pharmacology Fast Forward. Published on November 2, 2010 as DOI: 10.1124/mol.110.069013
This article has not been copyedited and formatted. The final version may differ from this version.

RESULTS

Validation of the model cell lines

This study aims to determine the effect of cortical actin on Mrp1/MRP1 (Abcc1/ABCC1) localization and function and relies on the use of two model cell lines that express active Mrp1 (Abcc1) or MRP1 (ABCC1). Neuro-2a cells express endogenous murine Mrp1 (Abcc1), while hamster BHK-MRP1 cells strongly express human MRP1 (ABCC1) as a result of transfection. If Mrp1/MRP1 (Abcc1/ABCC1) is sensitive to cortical actin disruption in both cell lines, this would indicate that the effect is not cell-type specific. We used CFDA as a substrate to measure Mrp1/MRP1 (Abcc1/ABCC1) activity. Its efflux from Neuro-2a cells (Figure 1A) was effectively inhibited by the Mrp/MRP-specific inhibitor MK571. When using the Pgp (Abcb1) inhibitor cyclosporin A, less inhibition of CFDA efflux was observed in Neuro-2a cells (Figure 1A). With the Pgp (Abcb1) substrate rhodamine 123 very little efflux activity was observed and there was little or no effect of cyclosporin A or MK571 (Figure 1A). This indicates that with CFDA as a substrate we measure Mrp (Abcc) activity in these cells. With the CFDA assay we can not discriminate between various members of the Mrp (Abcc) subfamily. Therefore, we performed RT-PCR to analyze the Mrp (Abcc) mRNA expression profile in Neuro-2a cells. Of the 7 subfamily members that were tested, Neuro-2a cells only expressed Mrp1 (Abcc1) (Figure 1C). Thus, potential interfering effects of other Mrps (Abccs) in efflux assays using CFDA as a substrate are minimized. Moreover, in accordance with the absence of rhodamine 123 efflux, the two murine forms of Pgp (Abcb1), i.e. Mdr1a (Abcb1a) and Mdr1b (Abcb1b) were not expressed in Neuro-2a cells (Figure 1C). In BHK-MRP1 cells RT-PCR could not be performed due to the lack of cDNA sequence information of the Mrps (Abccs) in these hamster cells. However, due to the forced expression, BHK-MRP1 cells displayed a drastically higher level of MRP1 than the level of Mrp1 in Neuro-2a cells (Figure 1D). Moreover, CFDA efflux from BHK-MRP1 cells was

Molecular Pharmacology Fast Forward. Published on November 2, 2010 as DOI: 10.1124/mol.110.069013
This article has not been copyedited and formatted. The final version may differ from this version.

effectively inhibited by MK571 (Figure 1B). Therefore, it is reasonable to assume that efflux of CFDA in these cells can be attributed to MRP1.

Cortical actin stabilizes lipid raft localization and function of Mrp1 (Abcc1) *in Neuro-2a cells*

A large group of Neuro-2a cells was imaged at two different focal planes in the z-direction, one focal plane for visualization of stress fibres and the other focal plane for visualization of cortical actin. The actin cytoskeleton is organized in such a way in these cells that the stress fibres occur mostly in the bottom part of the cells, where the cells are attached to the glass coverslip. The stress fibres are typically long fibres that extend from one membrane anchor point to another membrane anchor point on the opposite side of the cell. Upwards in the cells in z-direction the cortical actin becomes apparent. The cortical actin is localized close to the plasma membrane to support the membrane and provide tension to the membrane. By focusing the confocal laser microscope on a z-layer close to the glass coverslip we can image stress fibres in control Neuro-2a cells (Figure 2B; arrow head) and by focusing more up in the cells we can image cortical actin (Figure 2D; arrow). We employed two modulators of the actin cytoskeleton, latrunculin B and cytochalasin D. Treatment with 10 μM latrunculin B resulted in loss of both stress fibres and cortical actin (Figure 2, F and H, respectively). As a control, to show that we indeed focussed on the right z-layer, cells were stained for ezrin, which still is localized in the cortical region of the plasma membrane (Figure 2G). Upon treatment with 10 μg/ml cytochalasin D stress fibres were disrupted (Figure 2L), but cortical actin was still present (Figure 2N; arrow). Taken together, this shows that latrunculin B and cytochalasin D at the used concentrations affect cortical actin differently and makes these two modulators valuable tools for studying the role of cortical actin in function and localization of Mrp1 (Abcc1).

Molecular Pharmacology Fast Forward. Published on November 2, 2010 as DOI: 10.1124/mol.110.069013
This article has not been copyedited and formatted. The final version may differ from this version.

We used a detergent-free method for the isolation of lipid rafts and first characterized the gradient fractions in terms of cholesterol and sphingolipid enrichment. For this purpose, fractions 1-2 were pooled, as well as 3-4, 5-6 and 7-9. Fractions 1-2 were most strongly enriched in both cholesterol and sphingolipids (Figure 3), and to a lesser extent also fractions 3-4. This indicates that fractions 1-2, with the lowest buoyant density, optimally fulfil the criteria for lipid rafts. Latrunculin B, but not cytochalasin D treatment resulted in a shift of Mrp1 (Abcc1) out of lipid raft fractions in Neuro-2a cells (Figure 4A). Mrp1 (Abcc1) shifted from the lipid raft fractions 1-2 to the fractions 5-6, but mostly 7-9, all non-raft fractions (Figure 4B). Also Cav-1, an established lipid raft marker, displayed a shift out of lipid raft fractions upon latrunculin B treatment, but not upon cytochalasin D treatment (Figure 4A). Interestingly, actin was partly localized in lipid raft fractions in control cells, and also shifted from lipid rafts fractions in latrunculin B-treated, but not in cytochalasin D-treated cells (Figure 4A). Next we measured the efflux activity of Mrp1 (Abcc1). Efflux kinetics were determined (Figure 5A) and the efflux time of 5 minutes was chosen for all subsequent experiments on the impact of cytoskeleton modulators. Efflux inhibition by latrunculin B was concentration dependent (Figure 5B) and 10 μM was taken for subsequent experiments. Concomitant with a shift of Mrp1 (Abcc1) out of lipid rafts, its efflux function was reduced by latrunculin B treatment (Figure 5C). While latrunculin B strongly reduced Mrp1 (Abcc1)-mediated efflux, cytochalasin D was much less effective (Figure 5C). As a control experiment, we tested whether the agent latrunculin B inhibited Mrp1 efflux function as a direct competitive inhibitor (DCI). In this case Neuro-2a cells were not preincubated at 37^{o}C with latrunculin B, but the actin modulator was administered during the CFDA substrate loading period at 10^{o}C (DCI 1). Alternatively, latrunculin B was added just before the efflux commenced (DCI 2). Under both conditions latrunculin B could not exert its effect through actin modulation, but only by direct inhibition of Mrp1 function. However, loss of Mrp1

Molecular Pharmacology Fast Forward. Published on November 2, 2010 as DOI: 10.1124/mol.110.069013
This article has not been copyedited and formatted. The final version may differ from this version.

function was not observed (Figure 5D). Taken together, these results indicate that both Mrp1 (Abcc1) localization in lipid rafts and its functional activity as an efflux pump are dependent on intact cortical actin.

Cortical actin dependence of Mrp1/MRP1 (Abcc1/ABCC1) *localization and function is not cell type specific*

In BHK-MRP1 cells, a cell line which highly expresses human MRP1 (ABCC1), a similar effect of latrunculin B on MRP1 (ABCC1) localization in lipid raft fractions was observed (Figure 6A). MRP1 (ABCC1) shifted from the lipid raft fractions 1-2 to the non-raft fractions 5-6 (Figure 6B). Moreover, MRP1 (ABCC1)-mediated efflux was reduced by latrunculin B (Figure 7A). Again, cytochalasin D had a minor effect on both localization in lipid raft fractions and efflux function of MRP1 (ABCC1) (Figure 6, A and B; Figure 7A). Control BHK-MRP1 cells displayed stress fibres and cortical actin (Figure 8A). Latrunculin B (Figure 8C), but not cytochalasin D (Figure 8B), caused disruption of cortical actin. When BHK-MRP1 cells were treated with latrunculin B for 35 minutes, washed and further incubated for 15h in FCS-containing medium without latrunculin B, the actin cytoskeleton recovered (Figure 8D) and the cells displayed normal cell morphology and growth behavior. Concomitantly, the efflux activity of MRP1 (ABCC1) completely recovered (Figure 7A). Finally, jasplakinolide was employed to stabilize the actin cytoskeleton. BHK-MRP1 cells treated for 20h in medium without serum including this actin modulator showed normal morphology, stress fibres and cortical actin (Figure 8F) compared to control cells, that had been incubated for 20h in medium without serum (Figure 8E). In addition, jasplakinolide-treated cells displayed an accumulation of actin aggregates in the perinuclear region of the cells (Figure 8F). Upon jasplakinolide treatment, MRP1 (ABCC1)-mediated efflux was enhanced, opposite to the effect of latrunculin B (Figure 7B). In Neuro-2a cells a similar trend

Molecular Pharmacology Fast Forward. Published on November 2, 2010 as DOI: 10.1124/mol.110.069013
This article has not been copyedited and formatted. The final version may differ from this version.

was observed, but this effect was not significant (data not shown). MRP1 (ABCC1) association with lipid raft fractions was normal in jasplakinolide treated BHK-MRP1 cells, compared to control cells (Figure 6, A and B). Taken together, these results indicate that the effects of cortical actin on both Mrp1/MRP1 (Abcc1/ABCC1) localization in lipid rafts and its functional activity as an efflux pump are not cell type specific but occur in two different cell lines, Neuro-2a and BHK-MRP1, and thus can be generalized.

Cortical actin disruption leads to intracellular accumulation of Mrp1/MRP1 (Abcc1/ABCC1) So far we have established that latrunculin B reduces efflux activity of Mrp1/MRP1 (Abcc1/ABCC1) and this effect appears to be correlated with a shift of Mrp1/MRP1 (Abcc1/ABCC1) out of lipid rafts. To further investigate the subcellular localization of the ABC transporter under these conditions, we employed confocal microscopy. In control Neuro-2a cells, Mrp1 (Abcc1) is exclusively detected in the plasma membrane (Figure 9a, A and D). Here, Mrp1 (Abcc1) appears to partly colocalize with actin (Figure 9a, A-C), but not with Cav-1 (Figure 9a, D-F). After latrunculin B treatment, there is still strong plasma membrane staining of Mrp1 (Abcc1), but in addition some intracellular Mrp1 (Abcc1) is detected in the cell centre (Figure 9aL). This was not observed after cytochalasin D treatment (Figure 9aG), where Mrp1 (Abcc1) was detected exclusively in the plasma membrane and partly colocalized with actin (Figure 9a, G-K). Upon incubation with latrunculin B, Cav-1 displayed pronounced intracellular staining in the cell centre (Figure 9aM). Here, Mrp1 (Abcc1) and Cav-1 appeared to colocalize (Figure 9a, L-N). Apparently, intact cortical actin prevented intracellular appearance of Mrp1 (Abcc1) and accumulation of Cav-1. Similar results were obtained in BHK-MRP1 cells, where both MRP1 (ABCC1) and Cav-1 displayed increased intracellular staining upon latrunculin B treatment (Figure 9b, G-K), but not uopon cytochalasin D-treated cells (Figure 9b, D-F). However, in control BHK-MRP1 cells some

Molecular Pharmacology Fast Forward. Published on November 2, 2010 as DOI: 10.1124/mol.110.069013
This article has not been copyedited and formatted. The final version may differ from this version.

intracellular MRP1 (ABCC1) (and Cav-1) staining was readily observed (Figure 9b, A-C), in contrast to control Neuro-2a cells. This may be related to the forced expression of human MRP1 (ABCC1) in BHK-MRP1 cells. In view of these observations we continued our studies regarding Mrp1 (Abcc1) localization in Neuro-2a cells.

Intracellular localization of Mrp1 (Abcc1) *is due to increased endocytosis*

To investigate whether intracellular accumulation of Mrp1 (Abcc1) and Cav-1 was due to increased internalization of the proteins from the plasma membrane or alternatively impaired transport from the Golgi apparatus to the plasma membrane, we performed the following three experiments. First, immunolocalization with established markers for either Golgi (giantin) or endosomes (transferrin receptor) showed that intracellular Mrp1 (Abcc1) in latrunculin B-treated cells partly colocalized with the transferrin receptor (Figure 10, A-C), but not with giantin (Figure 10, D-F). This indicated that intracellular Mrp1 (Abcc1) was not a result of impaired transport out of the Golgi. Second, latrunculin B-treated cells were pre-treated and co-treated with 10 μM nocodazole to disrupt microtubules. If intracellular Mrp1 (Abcc1) originated from impaired exit from the Golgi, the intracellular labelling pattern would stabilize, given that biosynthetic trafficking from the Golgi apparatus to the plasma membrane is microtubule-dependent. However, intracellular Mrp1 (Abcc1) was not detected (Figure 11aD) and Cav-1 did not accumulate in the cell centre (Figure 11aH). The labelling pattern of Mrp1 (Abcc1) and Cav-1 resembled that of control cells (Figure 11a, A and E, respectively) as well as cells treated with 10 μM nocodazole (Figure 11a, C and G) and was largely different from that in latrunculin B-treated cells (Figure 11a, B and F). Also this result indicated that intracellular Mrp1 (Abcc1) localization was not due to impaired Golgi to plasma membrane trafficking. Rather, nocodazole pre-treatment prevented internalization of Mrp1 (Abcc1). Finally, to confirm endocytosis as the mechanism underlying intracellular

Molecular Pharmacology Fast Forward. Published on November 2, 2010 as DOI: 10.1124/mol.110.069013
This article has not been copyedited and formatted. The final version may differ from this version.

localization of Mrp1 (Abcc1) in latrunculin B-treated cells, tyrphostin A23 was used to inhibit the process of endocytosis. When latrunculin B-treated Neuro-2a cells were pre- and co-incubated with 300 μM tyrphostin A23, intracellular staining of Mrp1 (Abcc1) and Cav-1 was indeed not observed (Figure 12a, D and H, respectively). The labelling pattern resembled that of control cells (Figure 12a, A and E) as well as cells treated with 300 μM tyrphostin A23 (Figure 12a, C and G) and was largely different from that in latrunculin B-treated cells (Figure 12a, B and F). Taken together, these results indicate that latrunculin B-induced intracellular localization of Mrp1 (Abcc1) is due to increased endocytosis of the transporter from the plasma membrane.

Lipid rafts association, plasma membrane localization and efflux function of Mrp1 (Abcc1) *are coupled and depend on intact cortical actin*

As indicated, nocodazole pre-treatment appeared to prevent latrunculin B-induced internalization of Mrp1 (Abcc1). In accordance, under these conditions of combined treatment lipid raft association of Mrp1 (Abcc1) was largely intact and comparable to that in control cells (Figure 4, A and B). Moreover, with the combined treatment the efflux activity of Mrp1 (Abcc1) was comparable to that in control cells and substantially different from that in latrunculin B-treated cells (Figure 5C). It was therefore important to study the cortical actin status under these conditions. When applied separately, nocodazole disrupted microtubules without affecting cortical actin (Figure 11b, C and G versus A and E) and latrunculin B disrupted cortical actin without affecting microtubules (Figure 11b, B and F versus A and E). Interestingly, latrunculin B-treatment in combination with nocodazole and after nocodazole pre-treatment did not result in disruption of cortical actin (Figure 11b, D and H), but stress fibres were still sensitive to the inhibitor (not shown). Moreover, actin-lipid raft association under these conditions was comparable to control (Figure 4A).

Molecular Pharmacology Fast Forward. Published on November 2, 2010 as DOI: 10.1124/mol.110.069013
This article has not been copyedited and formatted. The final version may differ from this version.

Tyrphostin A23 prevents latrunculin B-induced Mrp1 (Abcc1) *internalization, but not reduced lipid raft association and efflux activity of the ABC transporter*

Also tyrphostin A23 was able to prevent latrunculin B-induced internalization of Mrp1 (Abcc1) (Figure 12a). Interestingly, this inhibitor of endocytosis was ineffective in preventing the other effects of latrunculin: Under the conditions of combined tyrphostin A23/latrunculin B treatment lipid raft association of Mrp1 (Abcc1) was reduced and comparable to that in latrunculin B treated cells (Figure 4, A and B). Tyrphostin A23 by itself somewhat reduced Mrp1 (Abcc1)-mediated efflux activity, but could not prevent the stronger latrunculin B-mediated effect on Mrp1 (Abcc1) activity (Figure 13). As expected, when latrunculin B-treated Neuro-2a cells were pre- and co-incubated with 300 μM tyrphostin A23 (Figure 12bD), the actin labelling pattern resembled that of latrunculin B treated cells (Figure 12bB). This indicated that pre- and co-treatment with tyrphostin A23 did not prevent latrunculin B-induced loss of cortical actin. Moreover, lipid raft association of actin was reduced under these conditions, comparable to the situation in cells which had been treated with latrunculin B alone (Figure 4A). In tyrphostin A23 treated cells cortical actin and also stress fibres remained intact (Figure 12bC), as in control cells (Figure 12bA).

Molecular Pharmacology Fast Forward. Published on November 2, 2010 as DOI: 10.1124/mol.110.069013
This article has not been copyedited and formatted. The final version may differ from this version.

DISCUSSION

In this study we have shown for the first time that cortical actin is involved in stabilizing Mrp1/MRP1 (Abcc1/ABCC1) in lipid rafts on the cell surface of two cell lines, Neuro-2a and BHK-MRP1. Neuro-2a cells have endogenous expression of Mrp1 (ABCC1), but not the related Mrp (Abcc) subfamily members 2-7. BHK-MRP1 is a cell line which stably expresses human MRP1 (ABCC1). In contrast to cytochalasin D, latrunculin B caused disruption of cortical actin, which is in agreement with other studies (e.g. Spector *et al.*, 1999) and loss of actin from lipid raft fractions. This resulted in a shift of Mrp1/MRP1 (Abcc1/ABCC1) out of lipid raft fractions and its internalization by endocytosis. Similar events were recorded for the lipid raft marker Cav-1. Likely, these were separate events, since Mrp1/MRP1 (Abcc1/ABCC1) did not appear to colocalize with Cav-1: Mrp1/MRP1 (Abcc1/ABCC1) displayed continuous fluorescence in the plasma membrane while Cav-1 presented with punctate fluorescence. This is in accordance with previous studies showing that ABC transporters are found in non-caveolar lipid rafts (Hinrichs *et al.*, 2004; Radeva *et al.*, 2005). Apparently, cortical actin was acting as a fence keeping raft-associated proteins from internalizing by endocytosis. For Cav-1 similar observations have been reported (Mundy *et al.*, 2002). Inward budding of membranes leading to the formation of endocytic vesicles, may well be stimulated by the loss of cortical actin, which normally confers elasticity on the plasma membrane (Ananthakrishnan *et al.*, 2006).

The Mrp1/MRP1 (Abcc1/ABCC1) activity is reduced concomitant with a shift out of lipid rafts and internalization of the ABC transporter. This suggests that lipid raft-cortical actin complexes provide the cell with a mechanism to stabilize Mrp1/MRP1 (Abcc1/ABCC1) function. We have shown this in Neuro-2a cells, which express endogenous (murine) Mrp1 and extended our observations to a different cell line, BHK-MRP1, which expresses human MRP1. In this context, previous studies have provided evidence for a functional link between

Molecular Pharmacology Fast Forward. Published on November 2, 2010 as DOI: 10.1124/mol.110.069013
This article has not been copyedited and formatted. The final version may differ from this version.

actin and two other ABC transporters, i.e. PGP (ABCB1) and MRP2 (ABCC2) (Bacso *et al.*, 2004; Luciani *et al.*, 2002; Kikuchi *et al.*, 2002). Therefore, actin association becomes a general theme in ABC transporter biology and may open new avenues for future therapeutic strategies to overcome MDR.

Our results obtained with nocodazole pre-treatment have three important implications. 1. They provide additional evidence that the intracellular accumulation of Mrp1 (Abcc1) in latrunculin B-treated cells is due to endocytosis and not to hampered biosynthetic transport out of the Golgi apparatus. 2. They provide additional evidence for the specific role of cortical actin in stabilizing Mrp1 (Abcc1) localization and function: All effects of latrunculin B treatment on Mrp1 (Abcc1) localization and function were prevented by nocodazole pre-treatment, since cortical actin was not disrupted under these conditions. Moreover, it shows that the effects of latrunculin B on Mrp1 (Abcc1) can not be attributed to a general toxic effect of latrunculin B, because this toxic effect would also occur after nocodazole treatment. 3. They suggest that effective cortical actin disruption by latrunculin B requires intact microtubules. Loss of sensitivity to latrunculin B is specific for cortical actin and not displayed by stress fibres. This suggests a function of microtubules in dynamic turnover of cortical actin.

The studies performed with the endocytosis inhibitor tyrphostin A23 have the following implications. 1. They once more show that intracellular accumulation of Mrp1 (Abcc1) is due to endocytosis. 2. With this tool we were able to disconnect the effects of latrunculin B on Mrp1 (Abcc1) internalization from its effects on lipid raft association and efflux activity.

In conclusion, cortical actin stabilizes Mrp1/MRP1 (Abcc1/ABCC1) in a lipid raft environment on the cell surface and supports optimal activity of this transporter as an efflux pump. We suggest that loss of the proper lipid raft environment in the context of cortical actin

Molecular Pharmacology Fast Forward. Published on November 2, 2010 as DOI: 10.1124/mol.110.069013
This article has not been copyedited and formatted. The final version may differ from this version.

results in loss of Mrp1/MRP1 (Abcc1/ABCC1) activity. Internalization of Mrp1 (Abcc1) does not appear to contribute of reduced activity, but could be a mechanism to remove inactive Mrp1 (Abcc1) molecules from the cell surface. This also implies that it is not the number of ABC transporter molecules on the cell surface that determines overall efflux activity, but rather the activity status of cell surface-resident Mrp1/MRP1 (Abcc1/ABCC1) molecules. This activity status in turn depends on properties of the specific membrane domain environment, including the presence of intact cortical actin.

Molecular Pharmacology Fast Forward. Published on November 2, 2010 as DOI: 10.1124/mol.110.069013
This article has not been copyedited and formatted. The final version may differ from this version.

ACKNOWLEDGEMENTS

Annie van Dam and Hjalmar Permentier (Mass Spectometry Core Facility, University of Groningen, A. Deusinglaan 1, 9713 AV Groningen, The Netherlands) are gratefully acknowledged for their help in the analysis of sphingolipids by liquid chromatography-electrospray ionization tandem mass spectrometry.

Molecular Pharmacology Fast Forward. Published on November 2, 2010 as DOI: 10.1124/mol.110.069013
This article has not been copyedited and formatted. The final version may differ from this version.

AUTHORSHIP CONTRIBUTION

Participated in research design: Hummel, and Kok

Conducted experiments: Hummel, Klappe, Ercan, and Kok

Contributed new reagents or analytic tools: not applicable

Performed data analysis: Hummel, Klappe, Ercan, and Kok

Wrote or contributed to the writing of the manuscript: Hummel, and Kok

Molecular Pharmacology Fast Forward. Published on November 2, 2010 as DOI: 10.1124/mol.110.069013
This article has not been copyedited and formatted. The final version may differ from this version.

References

Ananthakrishnan R, Guck J, Wottawah F, Schinkinger S, Lincoln B, Romeyke M, Moon T, and Käs J (2006) Quantifying the contribution of actin networks to the elastic strength of fibroblasts. *J. Theor. Biol.* **242**: 502-516.

Bacso Z, Nagy H, Goda K, Bene L, Fenyvesi F, Matko J, and Szabo G (2004) Raft and cytoskeleton associations of an ABC transporter: P-glycoprotein. *Cytometry A* **61**: 105-116.

Bligh EG, and Dyer WJ (1959) A rapid method of total lipid extraction and purification. *Can. J. Biochem. Physiol.* **37**: 911-917.

Brown DA, and London E (2000) Structure and function of sphingolipid- and cholesterol-rich membrane rafts. *J. Biol. Chem.* **275:** 17221-17224.

Chang X-B, Hou Y-X, and Riordan JR (1997) ATPase activity of purified multidrug resistance-associated protein. *J. Biol. Chem.* **272**: 30962-30968.

Chichili GR, and Rodgers W (2007) Clustering of membrane raft proteins by the actin cytoskeleton. *J. Biol. Chem.* **282**: 36682-36691.

Dudeja PK, Anderson KM, Harris JS, Buckingham L, and Coon JS (1995) Reversal of multidrug resistance phenotype by surfactants: relationship to membrane lipid fluidity. *Arch. Biochem. Biophys.* **319:** 309-315.

Gamble W, Vaughan M, Kruth HS, and Avignan J (1978) Procedure for determination of free and total cholesterol in micro- or nanogram amounts suitable for studies with cultured cells. *J. Lipid Res.* **19**: 1068-1070.

Hinrichs JWJ, Klappe K, Hummel I, and Kok JW (2004) ATP-binding cassette transporters are enriched in non-caveolar detergent-insoluble glycosphingolipid-enriched membrane domains (DIGs) in human multidrug-resistant cancer cells. *J. Biol. Chem.* **279:** 5734-5738.

Kikuchi S, Hata M, Fukumoto K, Yamane Y, Matsui T, Tamura A, Yonemura S, Yamagishi H, Keppler D, and Tsukita S (2002) Radixin deficiency causes conjugated hyperbilirubinemia with loss of Mrp2 from bile canalicular membranes. *Nat. Genetics* **31**: 320-325.

Lavie Y, Fiucci G, and Liscovitch M (1998) Up-regulation of caveolae and caveolar constituents in multidrug-resistant cancer cells. *J. Biol. Chem.* **273 :** 32380-32383.

Luciani F, Molinari A, Lozupone F, Calcabrini A, Lugini L, Stringaro A, Puddu P, Arancia G, Cianfriglia M, and Fais S (2002) P-glycoprotein-actin association through ERM family proteins: A role in P-glycoprotein function in human cells of lymphoid origin. *Blood* **99**: 641-648.

Macdonald JL, and Pike LJ (2005) A simplified method for the preparation of detergent-free lipid rafts. *J. Lipid. Res*. **46**: 1061-1067.

Mundy DI, Machleidt T, Ying Y-S, Anderson RGW, and Bloom GS (2002) Dual control of caveolar membrane traffic by microtubules and the actin cytoskeleton. *J. Cell Sci.* **115**: 4327-4339.

Radeva G, Perabo J, and Sharom FJ (2005) P-Glycoprotein is localized in intermediate-density membrane microdomains distinct from classical lipid rafts and caveolar domains. *FEBS J*. **272**: 4924-4937.

Romsicki Y, and Sharom FJ (1999) The membrane lipid environment modulates drug interactions with the P-glycoprotein multidrug transporter. *Biochemistry 38***:** 6887-6896

Schroeder R, London E, and Brown DA (1994) Interactions between saturated acyl chains confer detergent resistance on lipids and GPI-anchored proteins: GPI-anchored proteins in liposomes and cells show similar behavior. *Proc. Natl. Acad. Sci.* **91:** 12130-12134.

Sinicrope FA, Dudeja PK, Bissonette BM, Safa AR, and Brasitus TA (1992) Modulation of P-glycoprotein-mediated drug transport by alterations in lipid fluidity of rat liver canalicular membrane vesicles. *J. Biol. Chem.* **267:** 24995-25002.

Smith PK, Krohn RI, Hermanson GT, Mallia AK, Gartner FH, Provenzano MD, Fujimoto EK, Goeke NM, Olson BJ, and Klenk DC (1985) Measurement of protein using bicinchoninic acid. *Anal. Biochem.* **150**: 76-85.

Spector I, Braet F, Shochet NR, and Bubb MR (1999) New anti-actin drugs in the study of the organization and function of the actin cytoskeleton. *Microsc. Res. Tech.* **47**: 18-37.

Sullards MC, and Merrill AH, Jr. (2001) Analysis of sphingosine 1-phosphate, ceramides, and other bioactive sphingolipids by high-performance liquid chromatography-tandem mass spectrometry. *Sci STKE* **67**: PL1.

Sullards MC, Wang E, Peng Q, and Merrill AH, Jr. (2003) Metabolomic profiling of sphingolipids in human glioma cell lines by liquid chromatography tandem mass spectrometry. *Cell. Mol. Biol.* **49**: 789-797.

Molecular Pharmacology Fast Forward. Published on November 2, 2010 as DOI: 10.1124/mol.110.069013
This article has not been copyedited and formatted. The final version may differ from this version.

FIGURE LEGENDS

Figure 1. Validation of the Mrp1/MRP1 model cell lines Neuro-2a and BHK-MRP1. A: The efflux activity of Mrp1 (Abcc1) during 5 minutes in Neuro-2a cells was measured under control conditions or upon inhibition by 20 μM MK571 or 10 μM cyclosporin A, using CFDA as substrate. The same was done for the efflux activity of Pgp (Abcb1) using rhodamine 123 (R123) as substrate. The 5 minutes fluorescence values are expressed as the percentage of 0 minutes (= 100%). Data represent the mean + SD of 3 independent experiments. B: The efflux activity of MRP1 (ABCC1) during 5 minutes in BHK-MRP1 cells was measured under control conditions or upon inhibition by 20 μM MK571, using CFDA as substrate. The 5 minutes fluorescence values are expressed as the percentage of 0 minutes (= 100%). Data represent the mean + SD of 3 independent experiments. C: The mRNA expression profile of Mrp (Abcc) subfamily members 1-7 and the Pgp (Abcb1) variants Mdr1a (Abcb1a) and Mdr1b (Abcb1b) was analyzed by RT-PCR in Neuro-2a cells (N) and the positive controls murine liver tissue (L) and murine kidney tissue (K). D: The expression of MRP1 and Mrp1 protein in BHK-MRP1 and Neuro-2a cells, respectively, was analyzed by Western blotting, using β-tubulin as loading control. Note that the same amount of protein (30 μg) of BHK-MRP1 cells loaded on gel results in a higher level of MRP1, as compared to the level of Mrp1 in Neuro-2a cells.

Figure 2. Disruption of actin by cytochalasin D is limited to stress fibres, while latrunculin B also disrupts cortical actin in Neuro-2a cells. Neuro-2a cells were untreated (CON; A-D), treated with 10 μM latrunculin B (LAT; E-H) or 10 μg/ml cytochalasin D (CYT; K-N). Cells were stained for ezrin (A,C,E,G,K,M) or actin (B,D,F,H,L,N). The left panel shows images of a z-layer, when focused on stress fibres, while in the right panel the focus was on cortical actin in the same cells. Note that cortical actin (arrows) remains in cytochalasin D-treated

Molecular Pharmacology Fast Forward. Published on November 2, 2010 as DOI: 10.1124/mol.110.069013
This article has not been copyedited and formatted. The final version may differ from this version.

cells, but is lost in latrunculin B-treated cells. Stress fibres (arrow head) are lost in both latrunculin B- and cytochalasin D-treated cells. bar, 20 μm.

Figure 3. Enrichment of cholesterol and sphingolipid relative to protein in detergent-free lipid raft gradients of Neuro-2a cells. Detergent-free lipid raft gradients were analyzed for cholesterol (open bars) and sphingolipid (closed bars) profile. These lipid classes were measured in pooled gradient fractions and are expressed relative to protein content of the pooled gradient fractions. To calculate the ratio cholesterol/protein and sphingolipid/protein, the values of % in the gradient of each, cholesterol, sphingolipids and protein, were used. This ratio is therefore without unit and represents the relative enrichment in gradient fractions of cholesterol and sphingolipids, respectively, relative to protein enrichment in the respective fractions. Data represent the mean + SD of 3 independent experiments. *Values are significantly ($P < 0.05$) different from the cholesterol/protein ratio of fractions 5-6 (non-lipid raft membrane fractions) as determined by Student's *t*-test. #Values are significantly ($P < 0.05$) different from the sphingolipid/protein ratio of fractions 5-6 (non-lipid raft membrane fractions) as determined by Student's *t*-test.

Figure 4. Disruption of cortical actin results in loss of lipid raft association of Mrp1 (Abcc1) in Neuro-2a cells. Neuro-2a cells were untreated (CON), treated with 10 μg/ml cytochalasin D (CYT), with 10 μM latrunculin B (LAT), with 10 μM nocodazole followed by 10 μM nocodazole + 10 μM latrunculin B (NOC/LAT), or with 300 μM tyrphostin A23 followed by 300 μM tyrphostin A23 + 10 μM latrunculin B (TYR/LAT). A: Lipid raft association of Mrp1 (Abcc1), Cav-1 and actin was analyzed under these conditions. The values indicate the percentage of the specific protein found in the lipid raft fractions (1-2), relative to the total of that protein in the entire gradient (9 fractions). Typical results taken from 3 independent

Molecular Pharmacology Fast Forward. Published on November 2, 2010 as DOI: 10.1124/mol.110.069013
This article has not been copyedited and formatted. The final version may differ from this version.

experiments are shown. B: Quantification of the distribution of Mrp1 (Abcc1) over de gradient fractions under these conditions.

Figure 5. Disruption of cortical actin results in reduced efflux function of Mrp1 (Abcc1) in Neuro-2a cells. Neuro-2a cells were untreated (CON), treated with 10 μg/ml cytochalasin D (CYT), with 10 μM latrunculin B (LAT), with 10 μM nocodazole (NOC) or with 10 μM nocodazole followed by 10 μM nocodazole + 10 μM latrunculin B (NOC/LAT). A: Efflux kinetics of CFDA in control Neuro-2a cells. The fluorescence values after various time periods of efflux are expressed as the percentage of 0 minutes (= 100%). Data represent the mean + SD of 3 independent experiments. B: Concentration dependent effect of latrunculin B on Mrp1 (Abcc1)-mediated efflux of CFDA during 5 minutes in Neuro-2a cells. The 5 minutes fluorescence values are expressed as the percentage of 0 minutes (= 100%). Data represent the mean + SD of 3 independent experiments. C: The efflux activity of Mrp1 (Abcc1) during 5 minutes was measured under conditions of cytoskeletal modulation, using CFDA as substrate. The 5 minutes fluorescence values are expressed as the percentage of 0 minutes (= 100%). Data represent the mean + SD of 3 independent experiments. * indicates values that are significantly different from control ($P < 0.05$, as determined by Student's *t*-test). # indicates that efflux of NOC/LAT-treated cells is significantly different from that of LAT-treated cells ($P < 0.05$, as determined by Student's *t*-test). D: The efflux activity of Mrp1 (Abcc1) during 5 minutes was measured under conditions of potential direct competitive inhibition (DCI) by latrunculin B. Latrunculin B was added during the CFDA loading period at 10^{o}C (DCI 1) or alternatively just before the efflux period commenced (DCI 2). The 5 minutes fluorescence values are expressed as the percentage of 0 minutes (= 100%). Data represent the mean + SD of 3 independent experiments. DCI 1 and DCI 2 values are not significantly different from control ($P > 0.05$, as determined by Student's *t*-test).

Molecular Pharmacology Fast Forward. Published on November 2, 2010 as DOI: 10.1124/mol.110.069013
This article has not been copyedited and formatted. The final version may differ from this version.

Figure 6. Disruption of cortical actin results in loss of lipid raft association of MRP1 (ABCC1) in BHK-MRP1 cells. BHK-MRP1 cells were untreated (CON), treated with 10 μg/ml cytochalasin D (CYT) for 35 min, with 10 μM latrunculin B (LAT) for 35 min or with 50 nM jasplakinolide (JAS) for 20h in medium without serum. A: Lipid raft association of MRP1 (ABCC1) was analyzed under various conditions. The values indicate the percentage of MRP1 (ABCC1) found in the lipid raft fractions (1-2), relative to the total of that protein in the entire gradient (9 fractions). Typical results taken from 3 independent experiments are shown. B: Quantification of the distribution of MRP1 (ABCC1) over de gradient fractions under these conditions.

Figure 7. Disruption of cortical actin results in reduced efflux function of MRP1 (ABCC1) in BHK-MRP1 cells. BHK-MRP1 cells were untreated (CON), treated with 10 μg/ml cytochalasin D (CYT) for 35 min, with 10 μM latrunculin B (LAT) for 35 min or with 50 nM jasplakinolide (JAS) for 20h in medium without serum. LAT-treated cells were allowed to recover (LAT recovery) for 15h in FCS-containing medium in the absence of latrunculin B. A: The efflux activity of MRP1 (ABCC1) during 5 minutes was measured under various conditions, using CFDA as substrate. The 5 minutes fluorescence values are expressed as the percentage of 0 minutes (= 100%). Data represent the mean + SD of 3 independent experiments. * indicates values that are significantly different from control ($P < 0.05$, as determined by Student's *t*-test). # indicates that efflux of the recovered LAT-treated cells is significantly different from that of LAT-treated cells ($P < 0.05$, as determined by Student's *t*-test). B: The efflux activity of MRP1 (ABCC1) during 5 minutes was measured in jasplakinolide-treated cells and compared to the respective control, i.e. cells incubated in medium without serum for 20 h. The 5 minutes fluorescence values are expressed as the

Molecular Pharmacology Fast Forward. Published on November 2, 2010 as DOI: 10.1124/mol.110.069013
This article has not been copyedited and formatted. The final version may differ from this version.

percentage of 0 minutes (= 100%). Data represent the mean + SD of 3 independent experiments. * indicates that efflux of JAS-treated cells is significantly higher than efflux of control cells ($P < 0.05$, as determined by Student's *t*-test).

Figure 8. Latrunculin reversibly disrupts cortical actin in BHK-MRP1 cells. BHK-MRP1 cells were untreated (CON), treated with 10 μg/ml cytochalasin D (CYT) for 35 min, with 10 μM latrunculin B (LAT) for 35 min or with 50 nM jasplakinolide (JAS) for 20h in medium without serum. LAT-treated cells were allowed to recover (LAT recovery) for 15h in FCS-containing medium in the absence of latrunculin B. Cells were stained for actin. Cortical actin (arrows) remains in cytochalasin D-treated cells (B), but is lost in latrunculin B-treated cells (C). Cells which have recovered from latrunculin B treatment (D), as well as jasplakinolide-treated cells (F) display normal morphology, stress fibres and cortical actin. Jasplakinolide-treated cells (F) in addition have accumulation of actin aggregates in the perinuclear region (arrowhead). bars, 10 μm.

Figure 9. a) Disruption of cortical actin results in internalization of Mrp1 (Abcc1) as well as the lipid raft marker Cav-1 in Neuro-2a cells. Neuro-2a cells were untreated (CON; A-F), treated with 10 μg/ml cytochalasin D (CYT; G-K), or treated with 10 μM latrunculin B (LAT; L-N). Cellular localization of Mrp1 (Abcc1) (A,D,G,L), actin (B,H) or Cav-1 (E,M) was analyzed by confocal microscopy under these conditions. (C,F,K,N) are the overlay images. In latrunculin B-treated cells (L), but not cytochalasin D-treated cells (G), Mrp1 (Abcc1) displays intracellular staining, where it appears to partly colocalize with Cav-1 (L-N). In control cells, Mrp1 (Abcc1) partly colocalizes with actin (arrows in C), but not with Cav-1 (arrows in F indicate either Mrp1 (Abcc1) or Cav-1). bar, 10 μm. **b**) Disruption of cortical actin results in internalization of MRP1 (ABCC1) as well as the lipid raft marker Cav-1 in

Molecular Pharmacology Fast Forward. Published on November 2, 2010 as DOI: 10.1124/mol.110.069013
This article has not been copyedited and formatted. The final version may differ from this version.

BHK-MRP1 cells. BHK-MRP1 cells were untreated (CON; A-C), treated with 10 μg/ml cytochalasin D (CYT; D-F), or treated with 10 μM latrunculin B (LAT; G-K). Cellular localization of MRP1 (ABCC1) (A,D,G) or Cav-1 (B,E,H) was analyzed by confocal microscopy under these conditions. (C,F,K) are the overlay images. In latrunculin B-treated cells (G), but not cytochalasin D-treated cells (D), MRP1 (ABCC1) displays enhanced intracellular staining, where it partly colocalizes with Cav-1 (G-K). In control cells, MRP1 (ABCC1) does not colocalize with Cav-1 in the plasma membrane (A-C). In contrast to control Neuro-2a cells (Figure 9aA), control BHK-MRP1 cells display some intracellular MRP1 (ABCC1) staining in the cell center (Figure 9bA). bar, 10 μm.

Figure 10. Intracellular Mrp1 (Abcc1) partly colocalizes with transferrin receptor, but not with giantin in Neuro-2a cells. Neuro-2a cells were treated with 10 μM latrunculin B (LAT). Cellular localization of Mrp1 (Abcc1) (A,D), transferrin receptor (TfR; B) or giantin (E) was analyzed by confocal microscopy under these conditions. (C,F) are the overlay images. bar, 10 μm.

Figure 11. a) Mrp1 (Abcc1) and Cav-1 do not accumulate intracellularly in latrunculin B-treated cells after pretreatment with nocodazole in Neuro-2a cells. Neuro-2a cells were untreated (CON; A,E), treated with 10 μM latrunculin B (LAT; B,F), treated with 10 μM nocodazole (NOC; C,G), or treated with 10 μM nocodazole followed by 10 μM nocodazole + 10 μM latrunculin B (NOC/LAT; D,H). Cellular localization of Mrp1 (Abcc1) (A-D) or Cav-1 (E-H) was analyzed by confocal microscopy under these conditions. bar, 10 μm. **b**) Cortical actin is not disrupted in latrunculin B-treated cells after pre-treatment with nocodazole in Neuro-2a cells. Neuro-2a cells were untreated (CON; A,E), treated with 10 μM latrunculin B (LAT; B,F), 10 μM nocodazole (NOC; C,G), or 10 μM nocodazole followed by 10 μM

Molecular Pharmacology Fast Forward. Published on November 2, 2010 as DOI: 10.1124/mol.110.069013
This article has not been copyedited and formatted. The final version may differ from this version.

nocodazole + 10 μM latrunculin B (NOC/LAT; D,H). Cells were stained for actin (A-D) and β-tubulin (E-H). The focus was on cortical actin in the these cells. Note that cortical actin (arrows) remains in latrunculin B-treated cells after pre-treatment with nocodazole. bar, 20 μm.

Figure 12. a) Mrp1 (Abcc1) and Cav-1 do not accumulate intracellularly in latrunculin B-treated cells after pretreatment with tyrphostin A23 in Neuro-2a cells. Neuro-2a cells were untreated (CON; A,E), treated with 10 μM latrunculin B (LAT; B,F), treated with 300 μM tyrphostin A23 (TYR; C,G) or treated with 300 μM tyrphostin A23, followed by 300 μM tyrphostin A23 + 10 μM latrunculin B (TYR/LAT; D,H). Cellular localization of Mrp1 (Abcc1) (A-D) or Cav-1 (E-H) was analyzed by confocal microscopy under these conditions. bar, 10 μm. **b**) Tyrphostin A23 does not prevent latrunculin B-induced loss of cortical actin. Neuro-2a cells were untreated (CON; A), treated with 10 μM latrunculin B (LAT; B), 300 μM tyrphostin A23 (TYR; C), or 300 μM tyrphostin A23 followed by 300 μM tyrphostin A23 + 10 μM latrunculin B (TYR/LAT; D). Cells were stained for actin. Note that cortical actin is disrupted in latrunculin B-treated cells (B) and also after pre-treatment with tyrphostin A23 (D). In tyrphostin A23-treated cells cortical actin and also stress fibres are intact (C), as in control cells (A). bar, 20 μm.

Figure 13. Tyrphostin A23 does not prevent latrunculin B-induced reduction of MRP-mediated efflux activity. Neuro-2a cells were untreated (CON), treated with 10 μM latrunculin B (LAT), 300 μM tyrphostin A23 (TYR), or 300 μM tyrphostin A23 followed by 300 μM tyrphostin A23 + 10 μM latrunculin B (TYR/LAT). The efflux activity of Mrp1 (Abcc1) during 5 minutes was measured under conditions of cytoskeleton and endocytosis

Molecular Pharmacology Fast Forward. Published on November 2, 2010 as DOI: 10.1124/mol.110.069013
This article has not been copyedited and formatted. The final version may differ from this version.

modulation, using CFDA as substrate. The 5 minutes fluorescence values are expressed as the percentage of 0 minutes (= 100%). Data represent the mean + SD of 3 independent experiments. * indicates values that are significantly different from control ($P < 0.05$, as determined by Student's *t*-test). n.s. indicates that efflux of TYR/LAT-treated cells is not significantly different from that of LAT-treated cells ($P > 0.05$, as determined by Student's *t*-test).

Molecular Pharmacology Fast Forward. Published on November 2, 2010 as DOI: 10.1124/mol.110.069013
This article has not been copyedited and formatted. The final version may differ from this version.

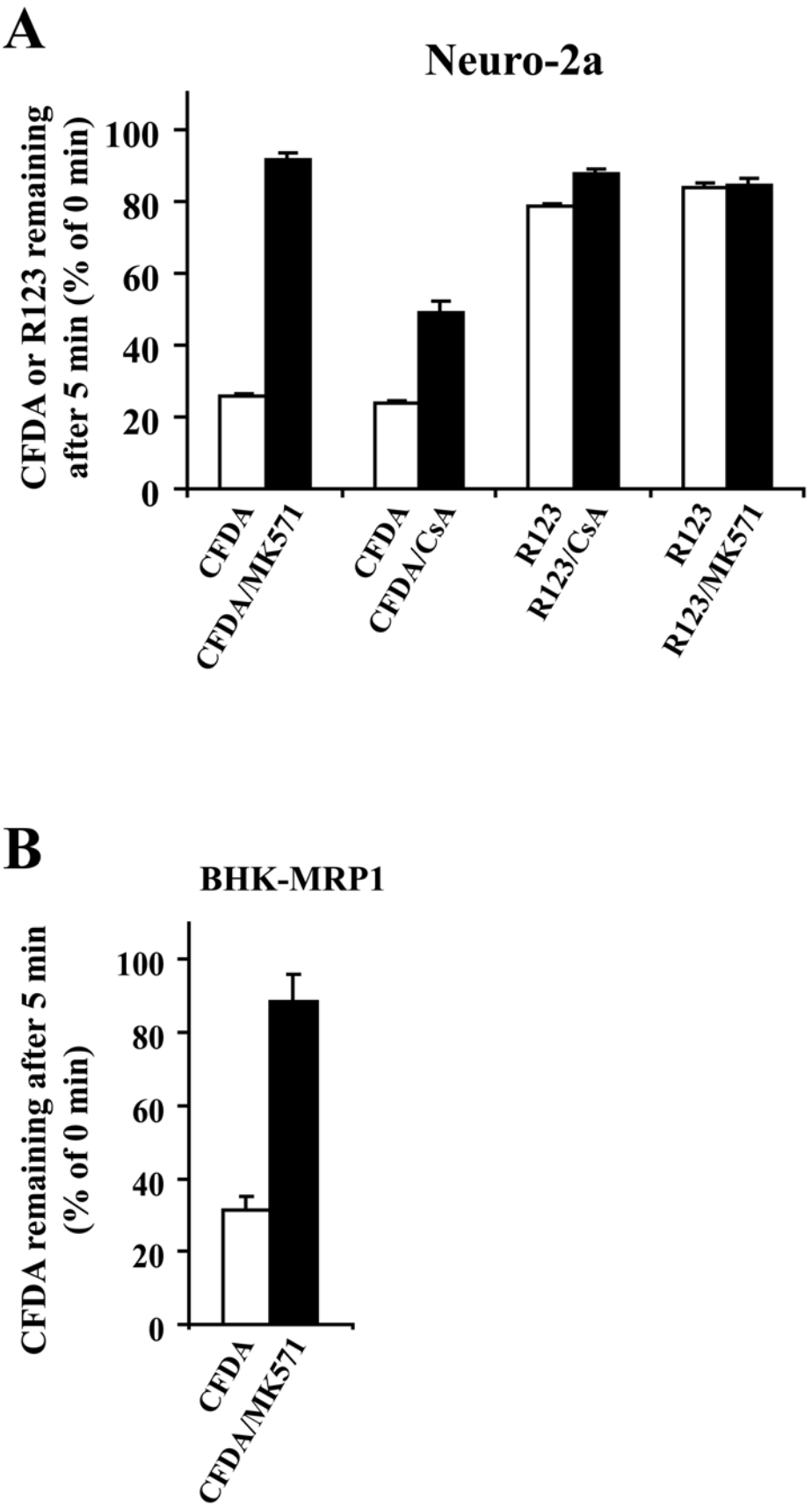

Figure 1

Molecular Pharmacology Fast Forward. Published on November 2, 2010 as DOI: 10.1124/mol.110.069013
This article has not been copyedited and formatted. The final version may differ from this version.

C

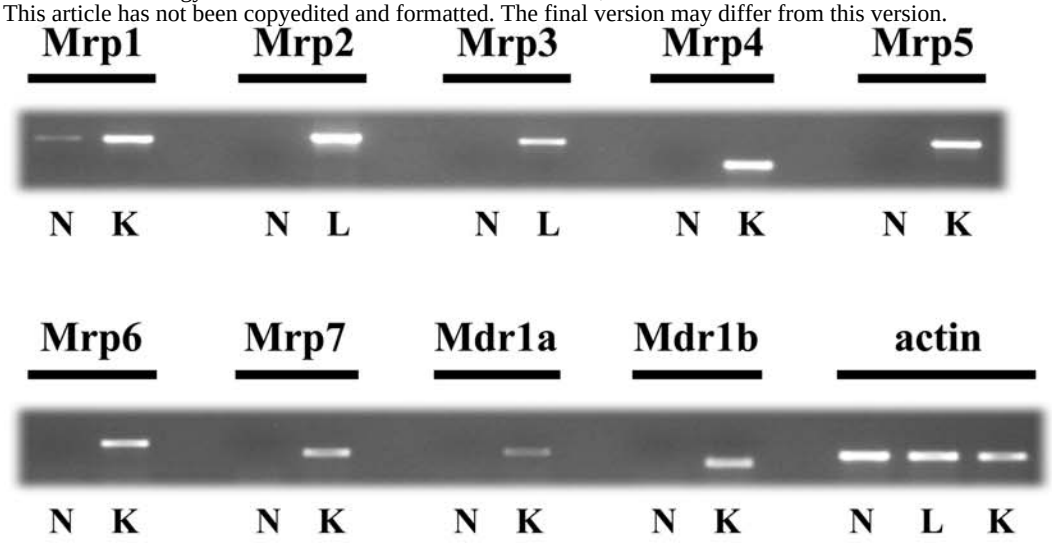

D

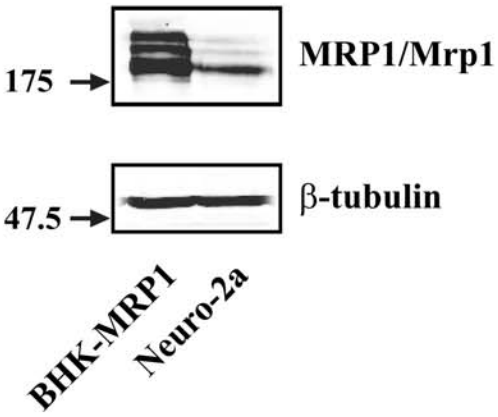

Figure 1

Molecular Pharmacology Fast Forward. Published on November 2, 2010 as DOI: 10.1124/mol.110.069013
This article has not been copyedited and formatted. The final version may differ from this version.

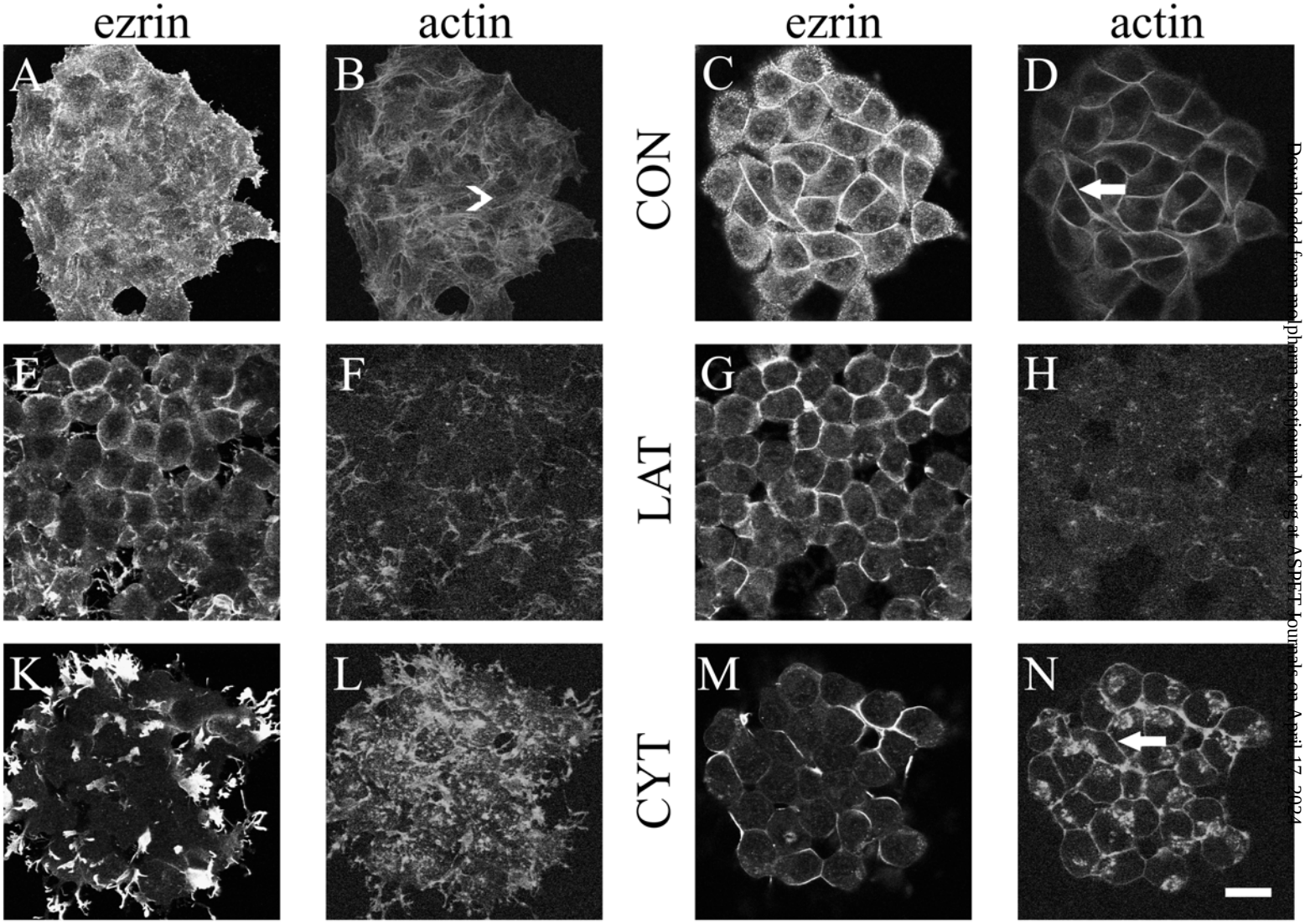

Figure 2

Molecular Pharmacology Fast Forward. Published on November 2, 2010 as DOI: 10.1124/mol.110.069013
This article has not been copyedited and formatted. The final version may differ from this version.

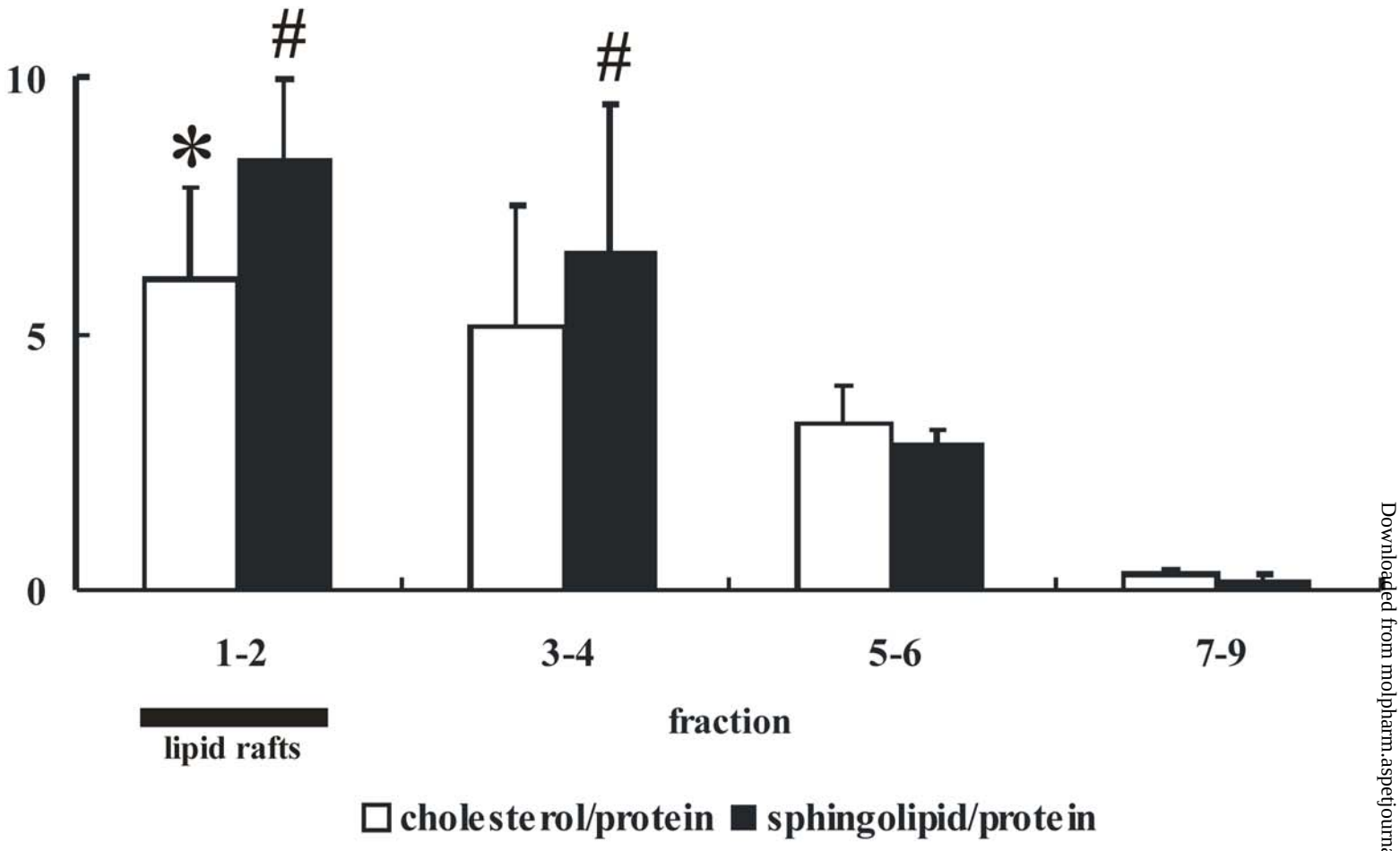

Figure 3

Molecular Pharmacology Fast Forward. Published on November 2, 2010 as DOI: 10.1124/mol.110.069013
This article has not been copyedited and formatted. The final version may differ from this version.

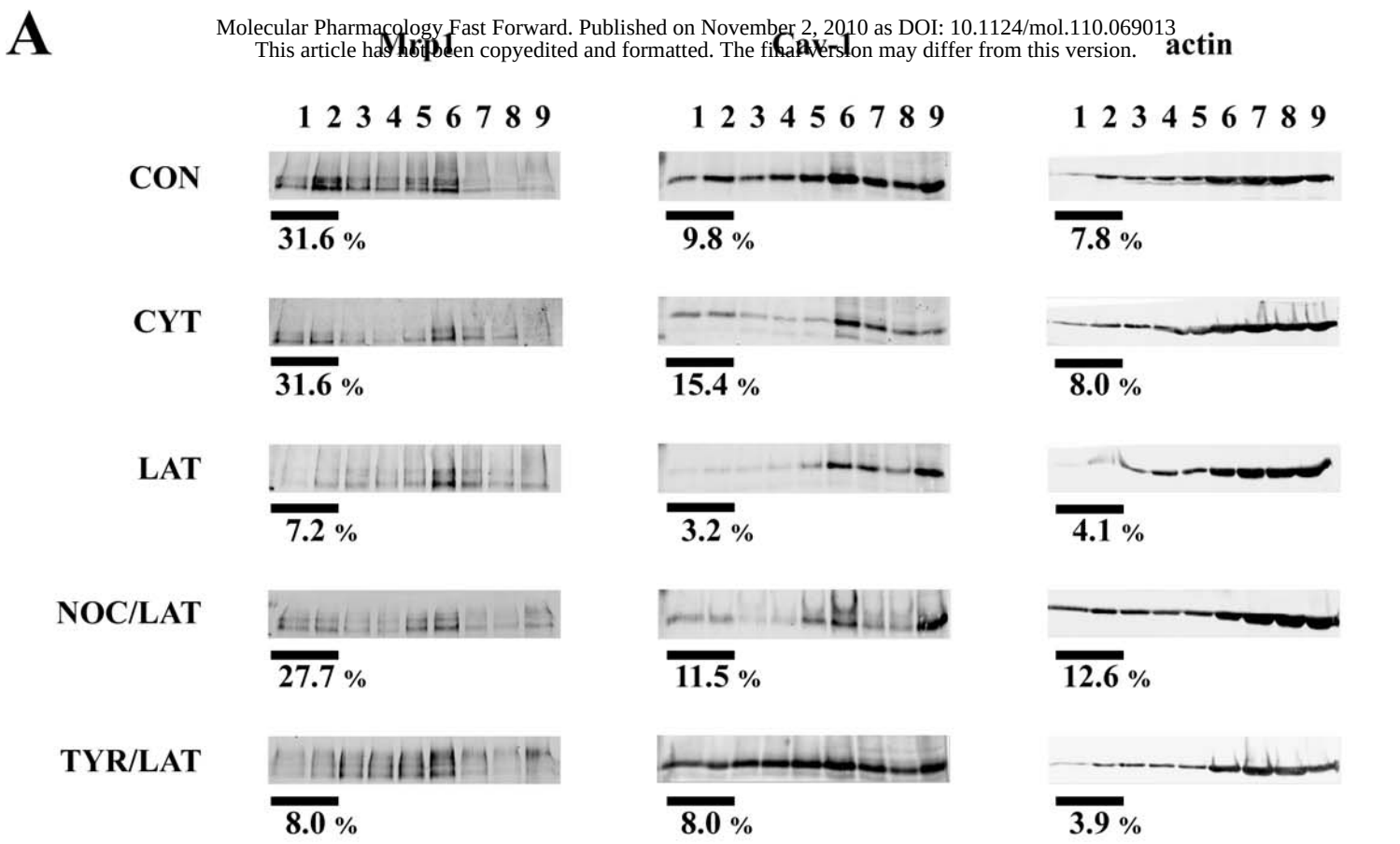

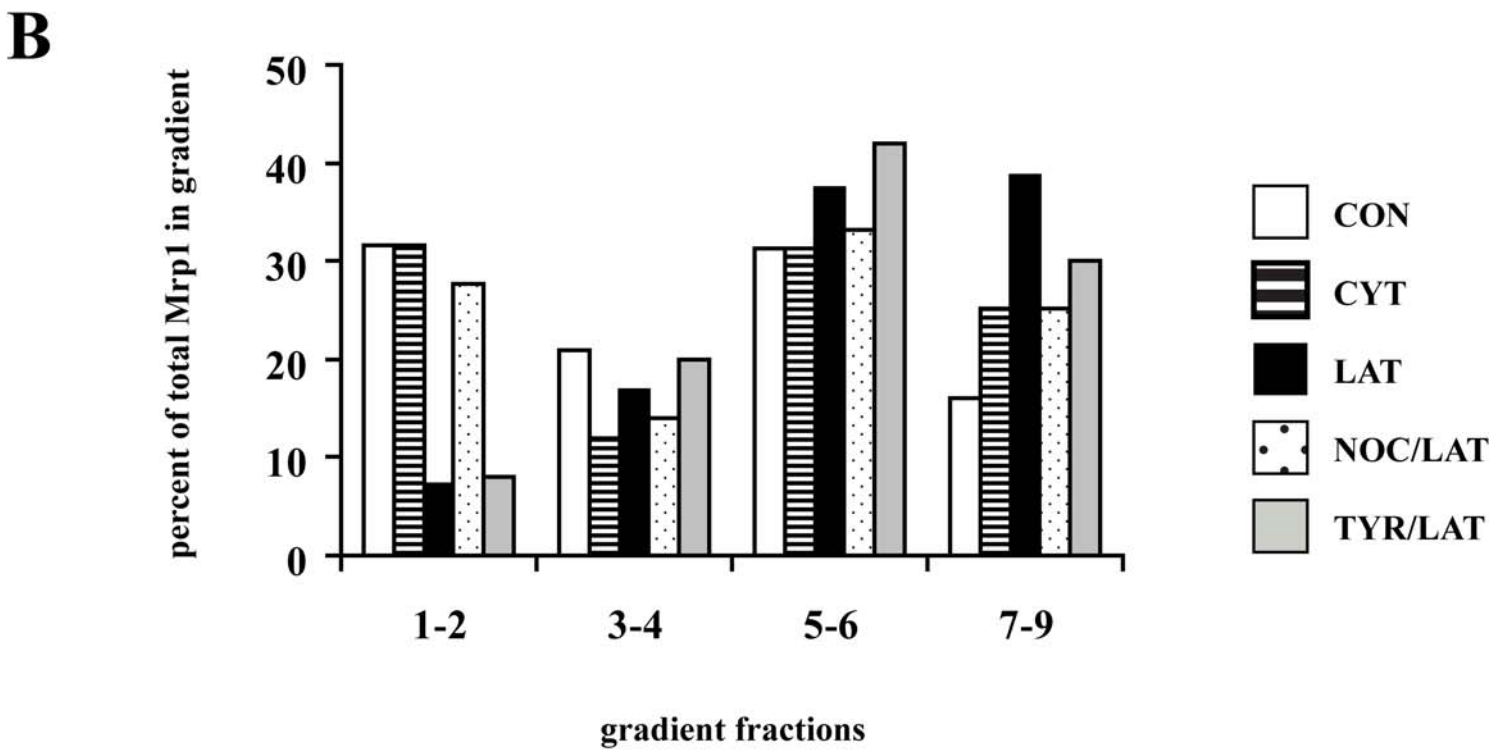

Figure 4

Molecular Pharmacology Fast Forward. Published on November 2, 2010 as DOI: 10.1124/mol.110.069013
This article has not been copyedited and formatted. The final version may differ from this version.

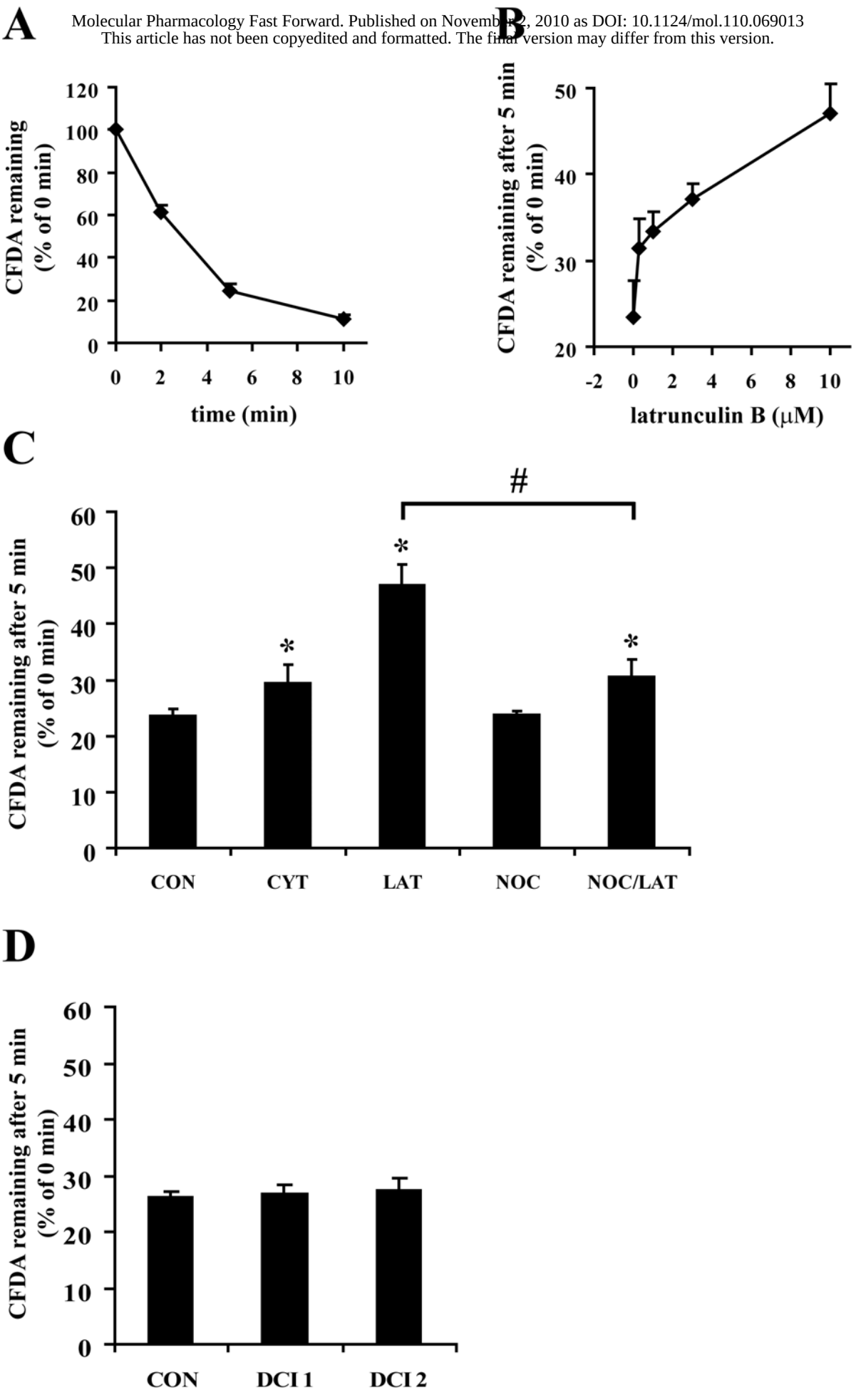

Figure 5

Molecular Pharmacology Fast Forward. Published on November 2, 2010 as DOI: 10.1124/mol.110.069013
This article has not been copyedited and formatted. The final version may differ from this version.

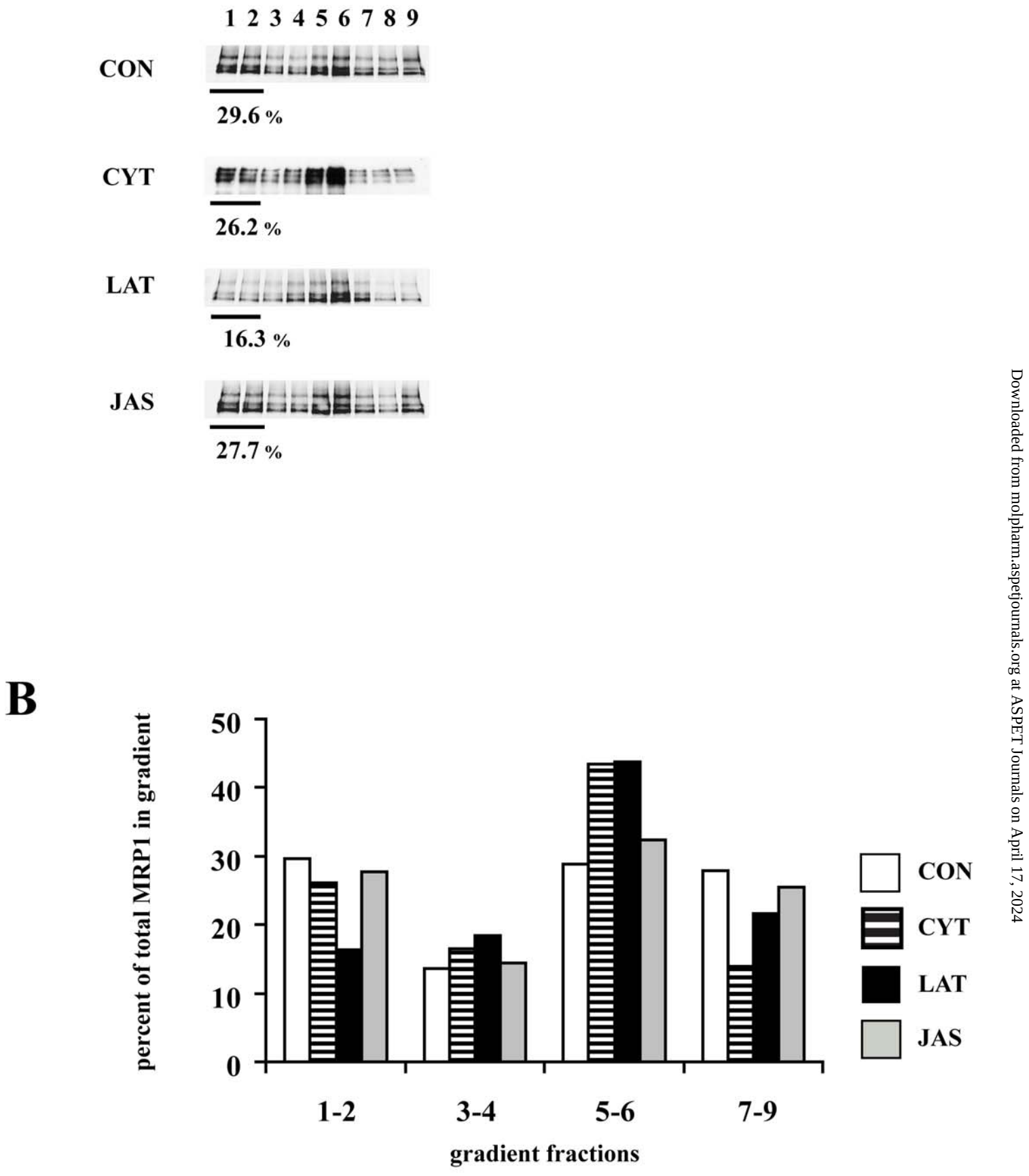

Figure 6

Molecular Pharmacology Fast Forward. Published on November 2, 2010 as DOI: 10.1124/mol.110.069013
This article has not been copyedited and formatted. The final version may differ from this version.

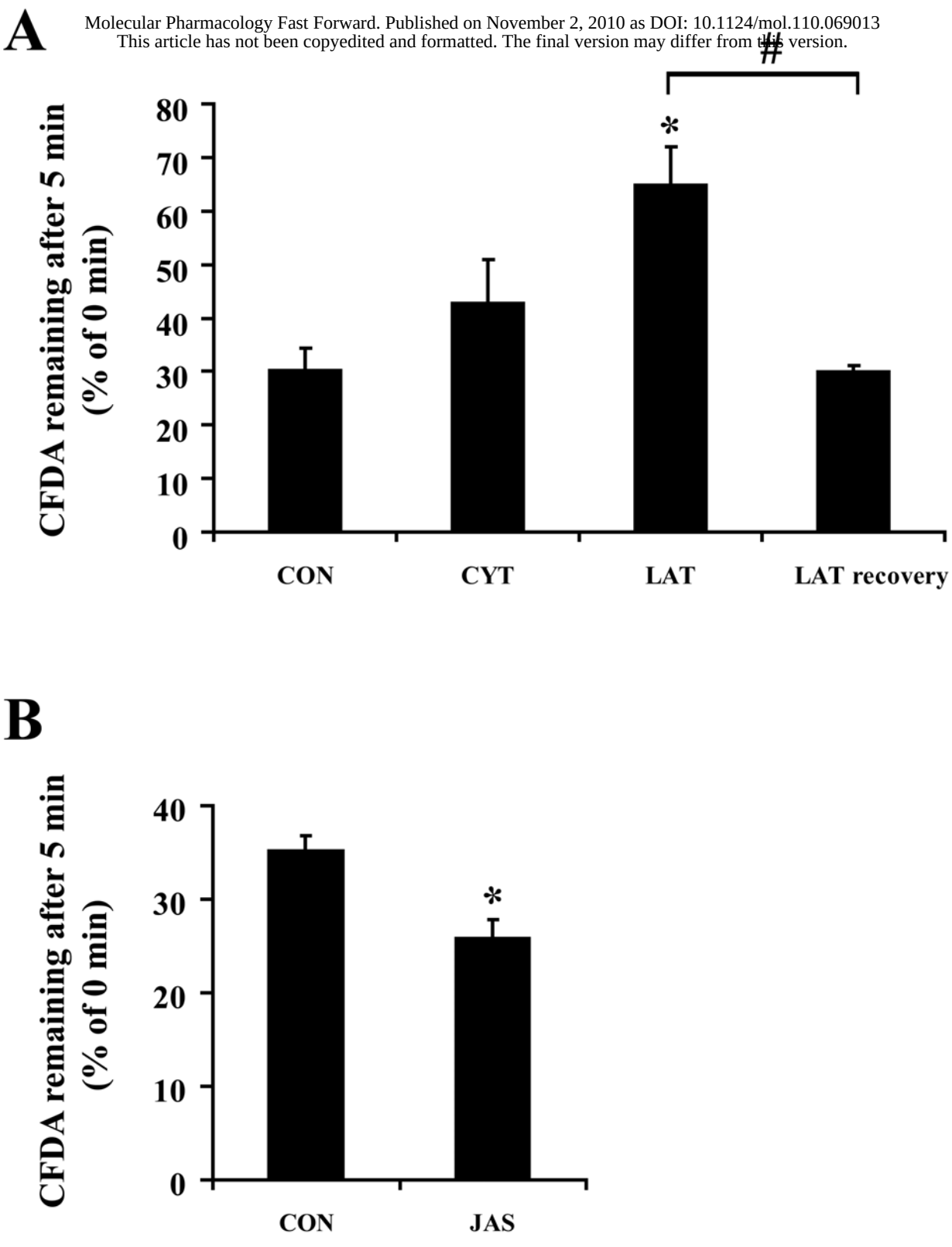

Figure 7

Molecular Pharmacology Fast Forward. Published on November 2, 2010 as DOI: 10.1124/mol.110.069013
This article has not been copyedited and formatted. The final version may differ from this version.

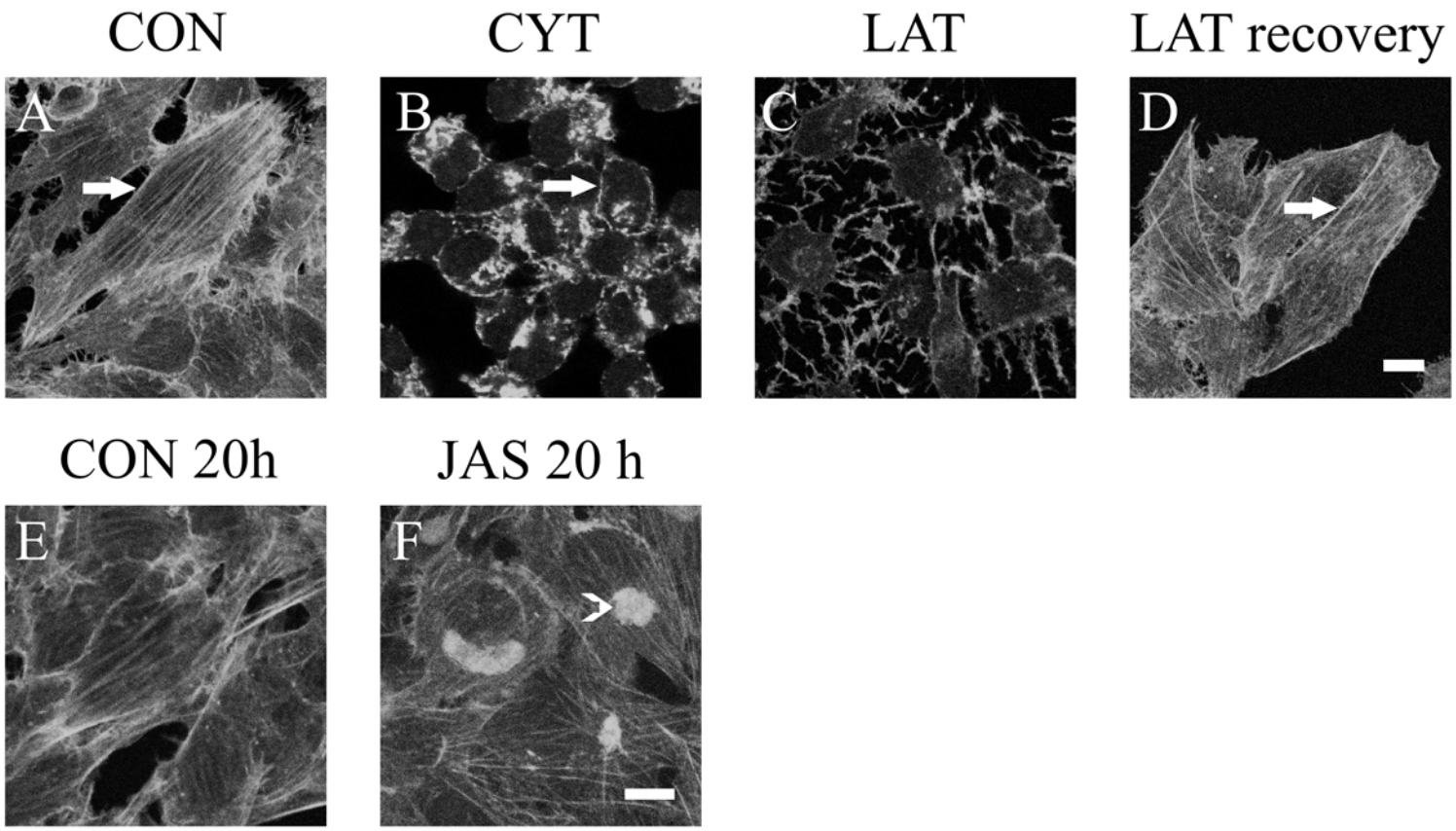

Figure 8

Molecular Pharmacology Fast Forward. Published on November 2, 2010 as DOI: 10.1124/mol.110.069013
This article has not been copyedited and formatted. The final version may differ from this version.

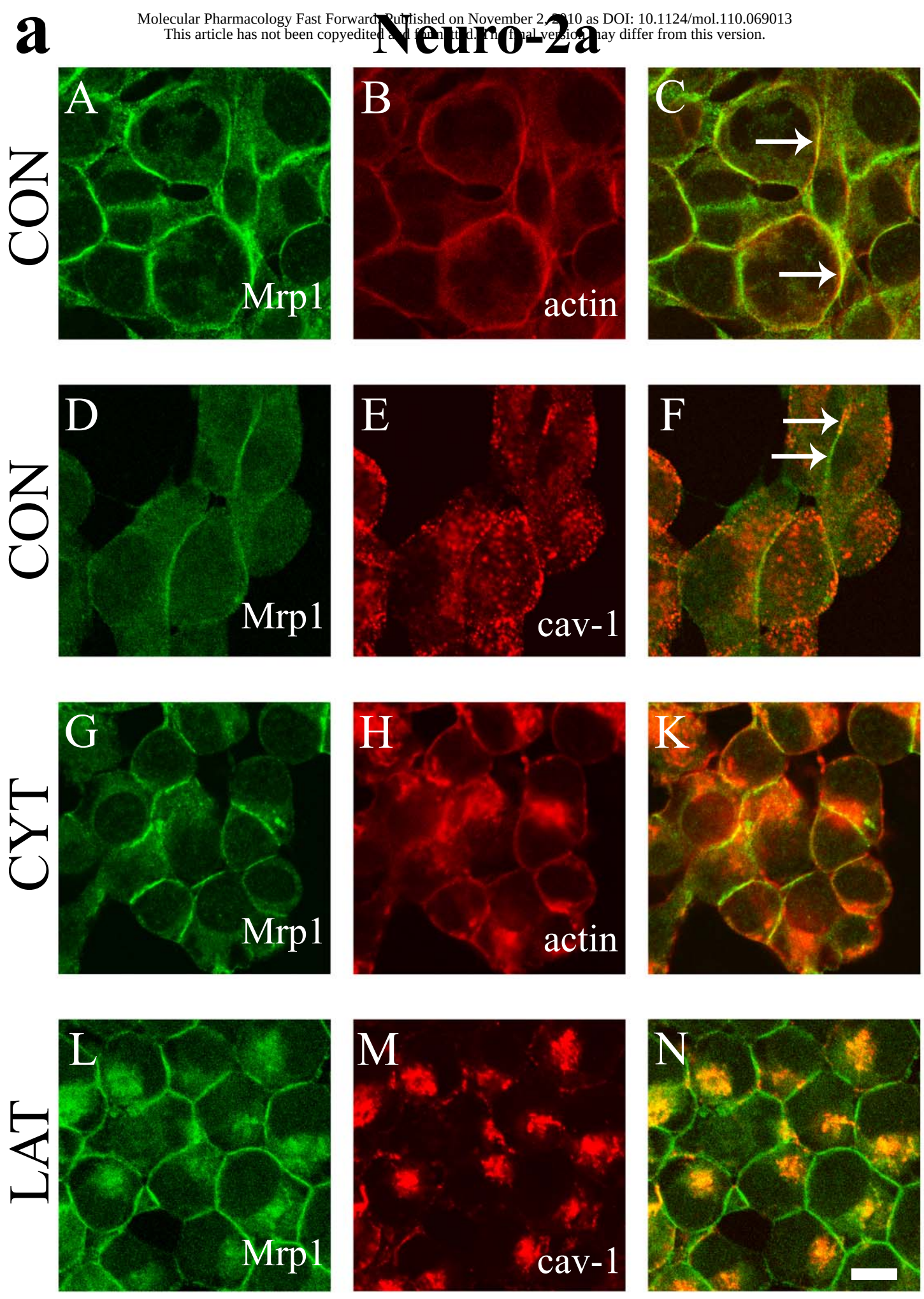

Figure 9

Molecular Pharmacology Fast Forward. Published on November 2, 2010 as DOI: 10.1124/mol.110.069013
This article has not been copyedited and formatted. The final version may differ from this version.

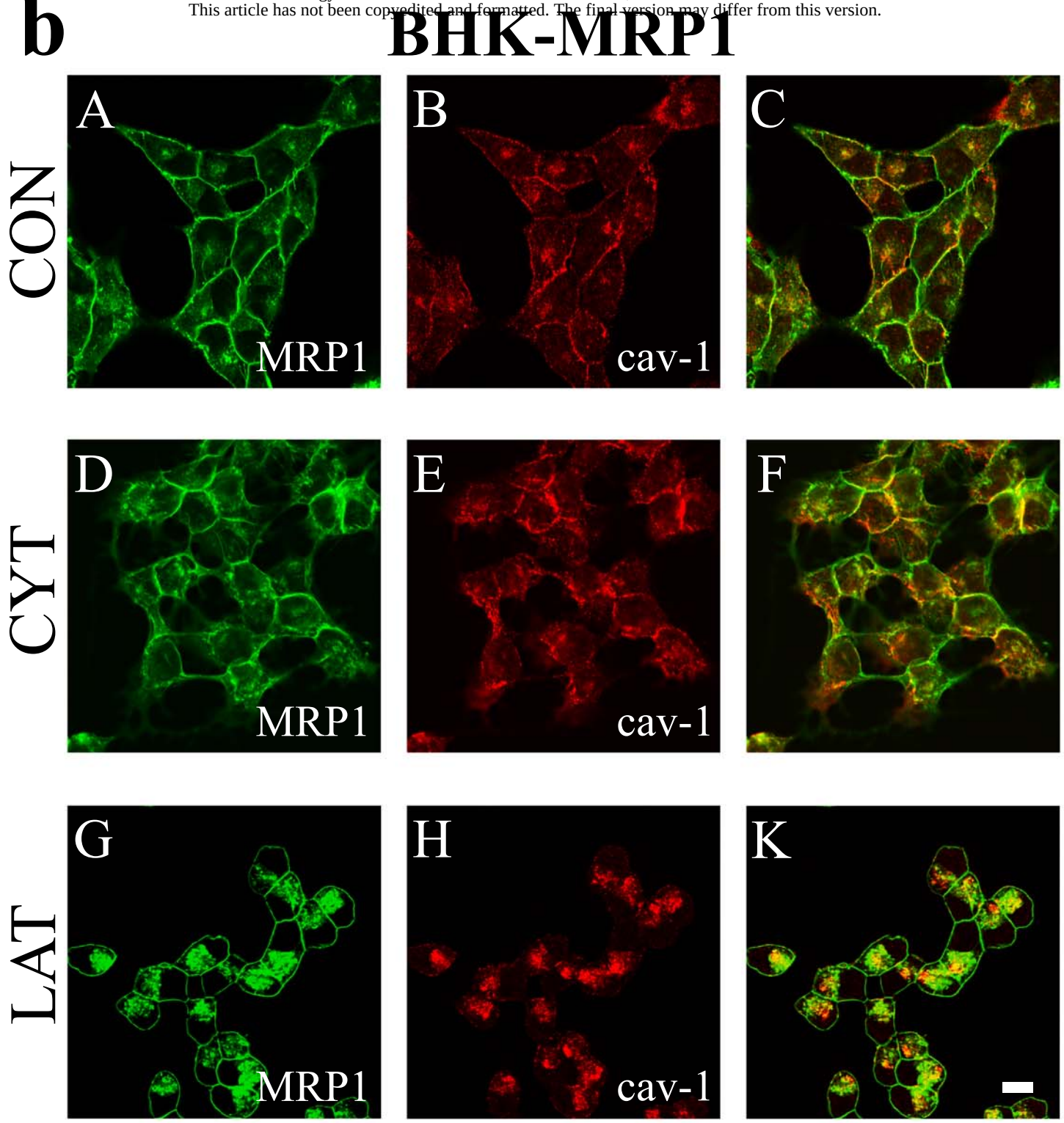

Figure 9

Molecular Pharmacology Fast Forward. Published on November 2, 2010 as DOI: 10.1124/mol.110.069013
This article has not been copyedited and formatted. The final version may differ from this version.

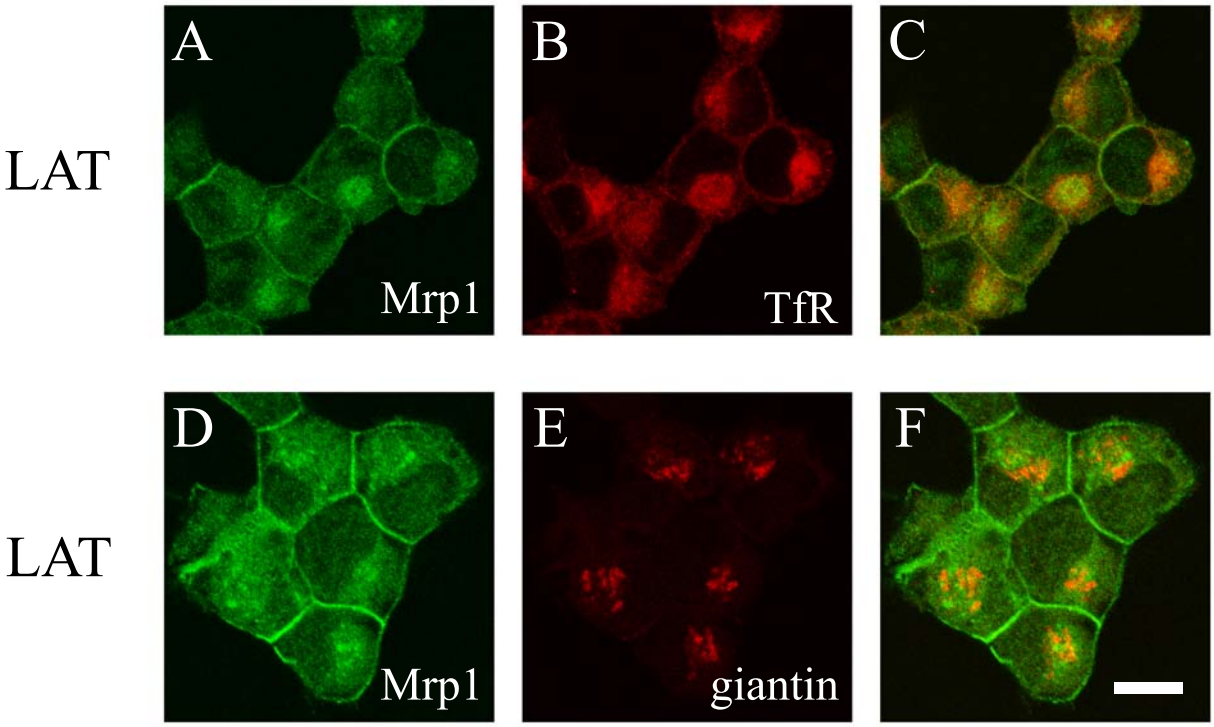

Figure 10

Molecular Pharmacology Fast Forward. Published on November 2, 2010 as DOI: 10.1124/mol.110.069013
This article has not been copyedited and formatted. The final version may differ from this version.

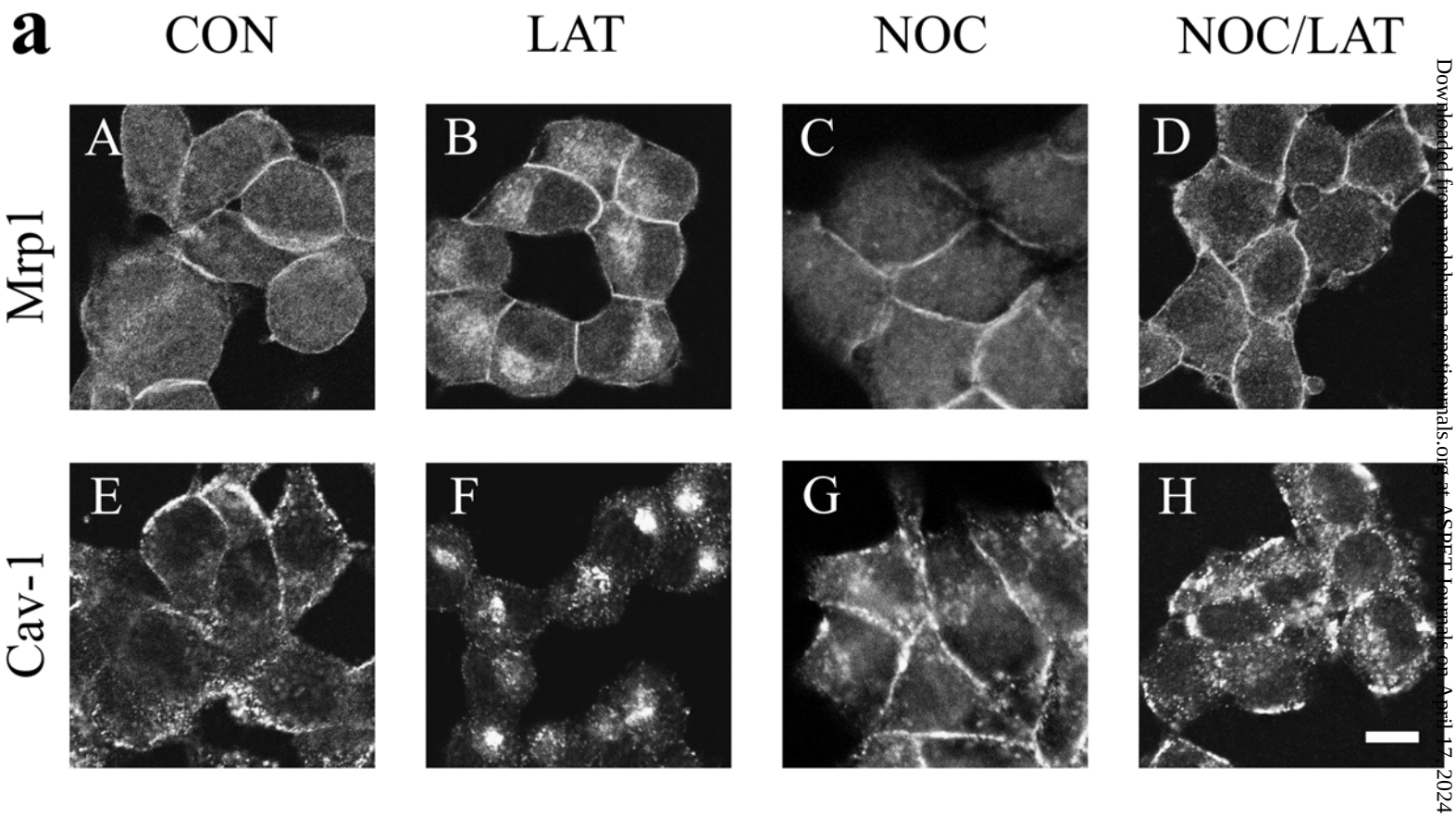

Figure 11

Molecular Pharmacology Fast Forward. Published on November 2, 2010 as DOI: 10.1124/mol.110.069013
This article has not been copyedited and formatted. The final version may differ from this version.

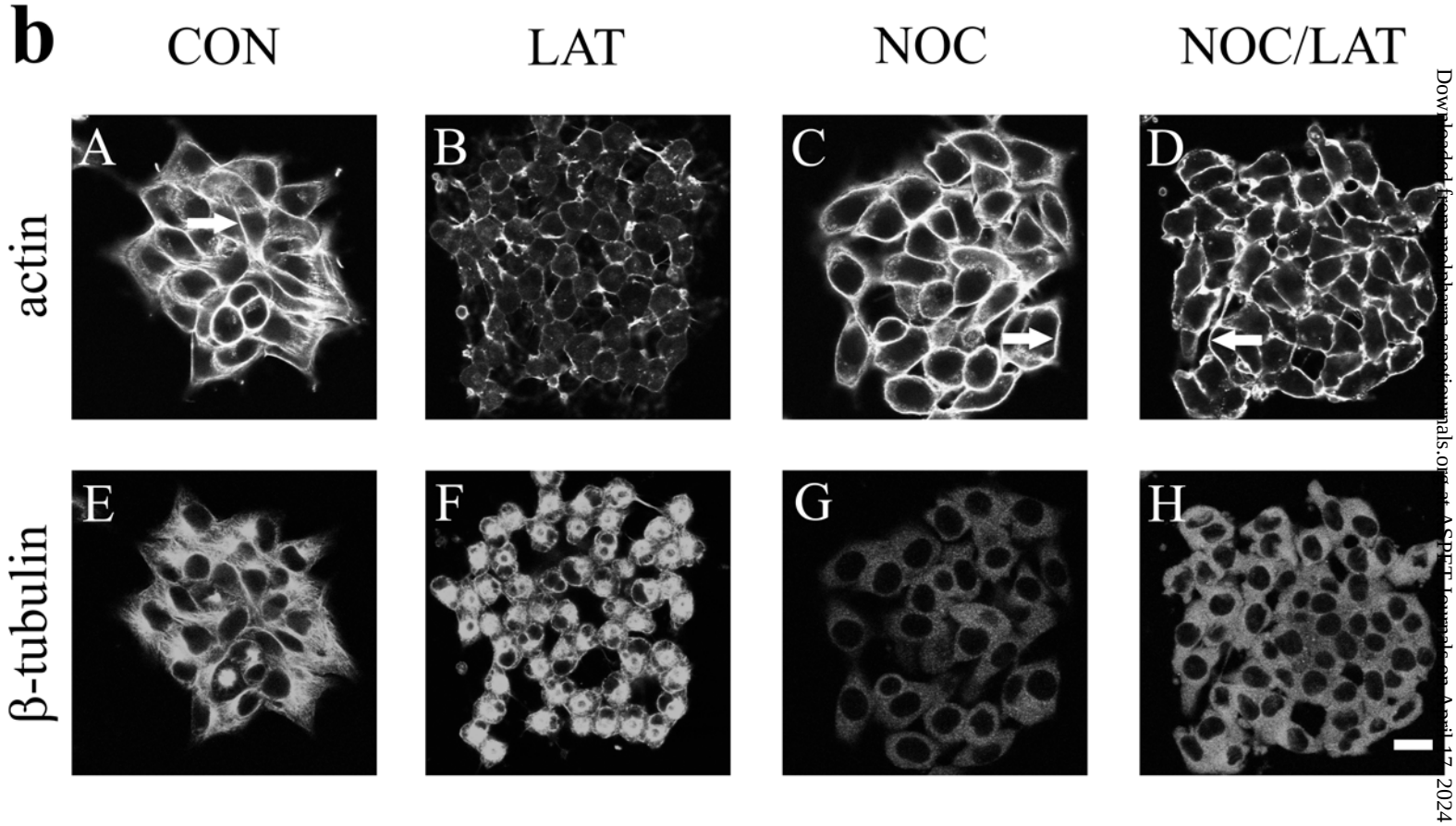

Figure 11

Molecular Pharmacology Fast Forward. Published on November 2, 2010 as DOI: 10.1124/mol.110.069013
This article has not been copyedited and formatted. The final version may differ from this version.

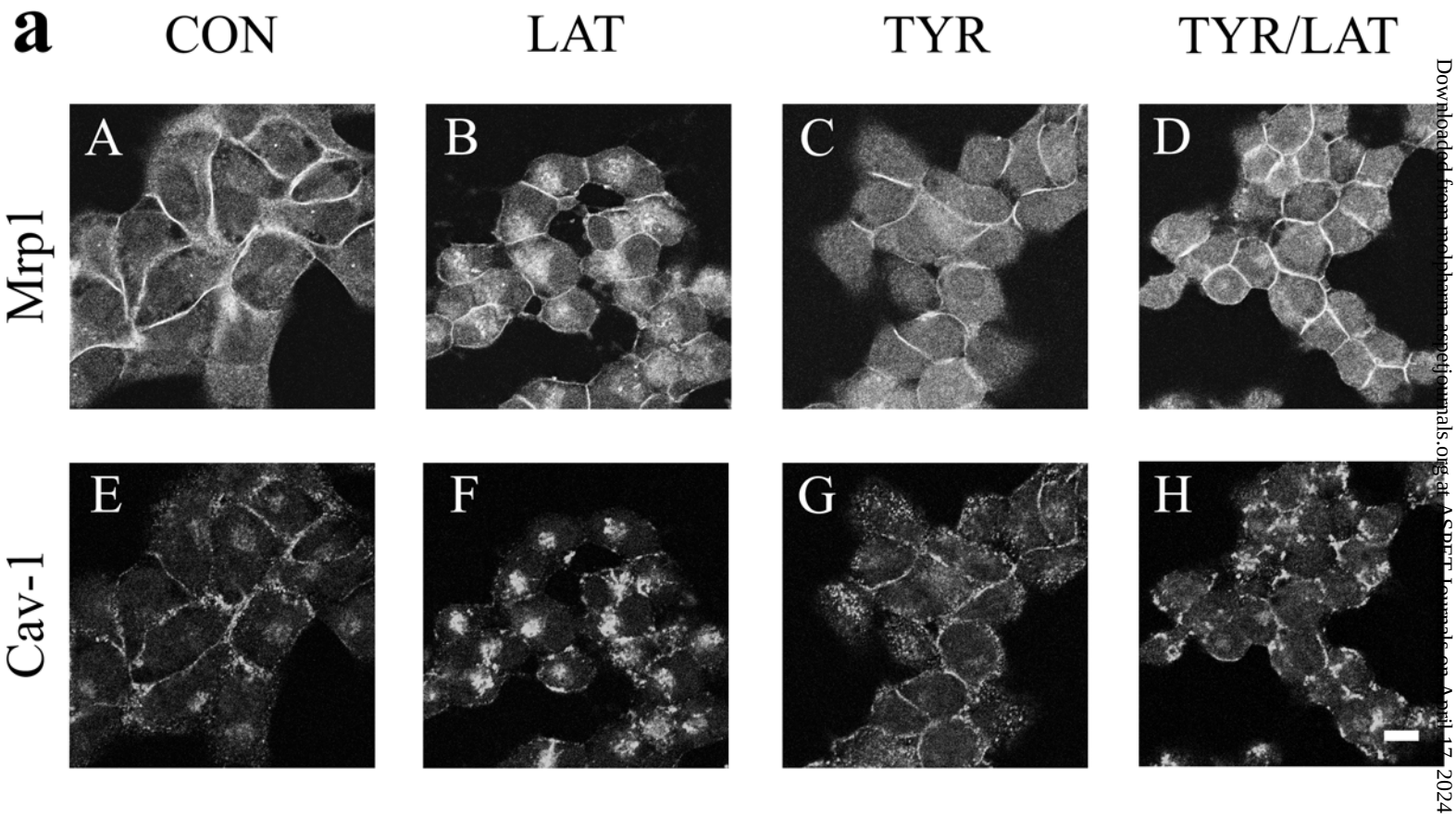

Figure 12

Molecular Pharmacology Fast Forward. Published on November 2, 2010 as DOI: 10.1124/mol.110.069013
This article has not been copyedited and formatted. The final version may differ from this version.

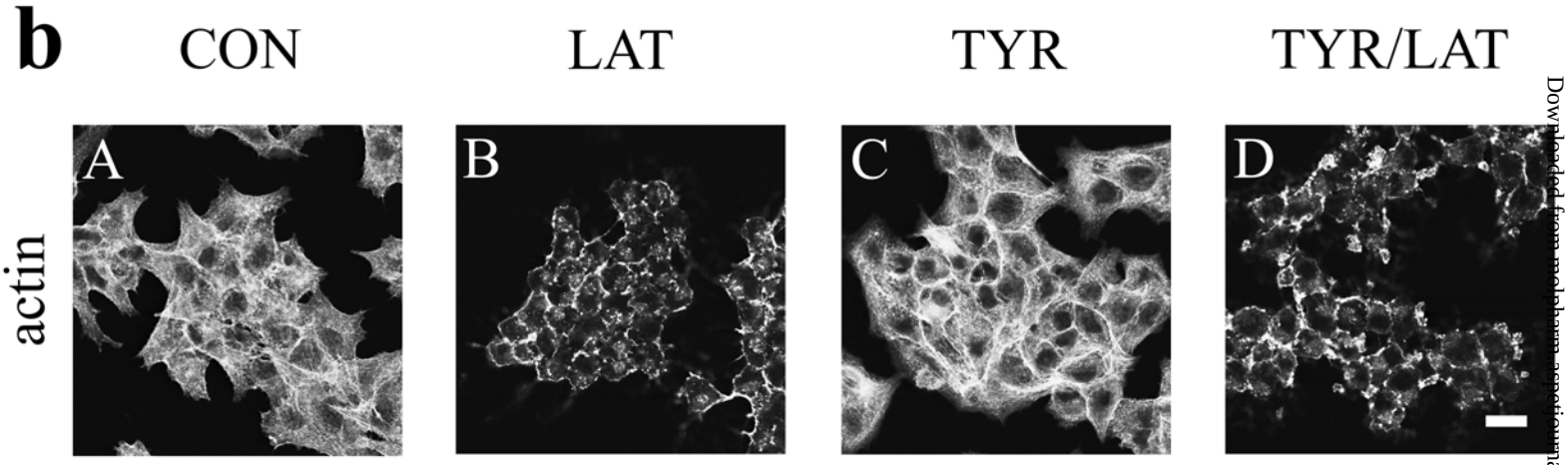

Figure 12

Molecular Pharmacology Fast Forward. Published on November 2, 2010 as DOI: 10.1124/mol.110.069013
This article has not been copyedited and formatted. The final version may differ from this version.

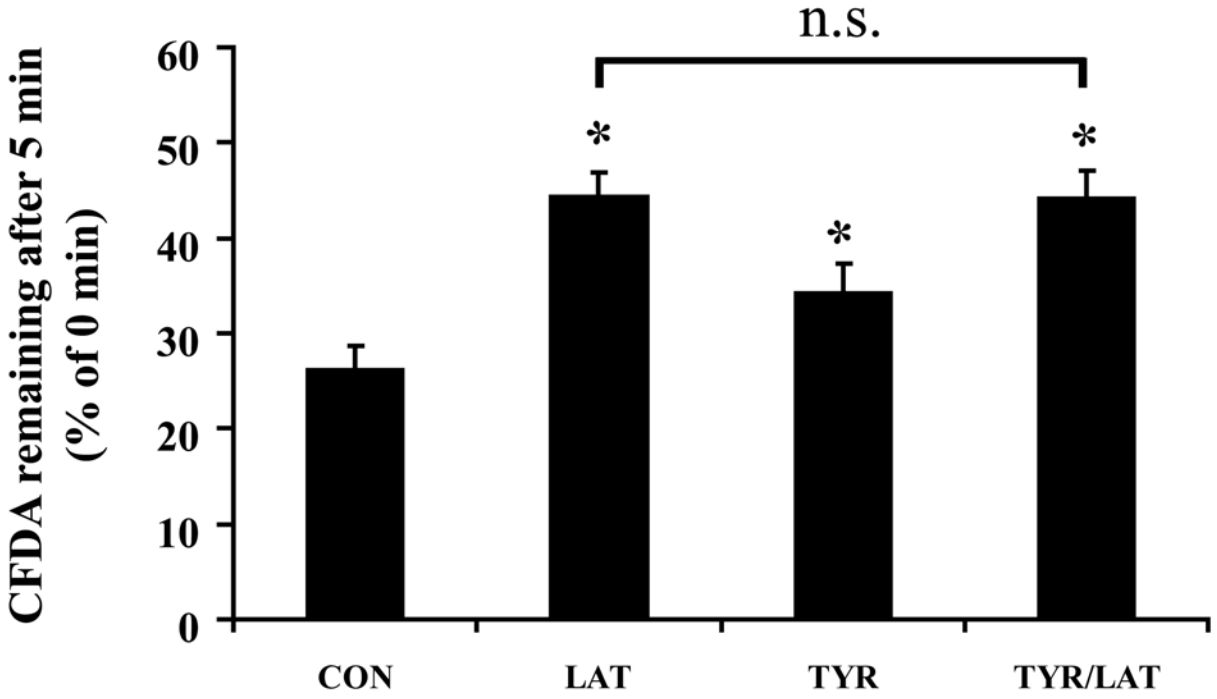

Figure 13